

# **DEVELOPMENT AND TESTING OF A NOVEL ANCHOR-PROFILED FRP JACKET SYSTEM FOR EFFECTIVE CONFINEMENT OF RECTANGULAR CONCRETE COLUMNS**

February  
2025

A Research Report from the Pacific Southwest  
Region University Transportation Center

Bora Gencturk, University of Southern California

Botong Zheng, University of Southern California



University Transportation Center



## TECHNICAL REPORT DOCUMENTATION PAGE

<b>1. Report No.</b> PSR-23-04 TO 074	<b>2. Government Accession No.</b> N/A	<b>3. Recipient's Catalog No.</b> N/A	
<b>4. Title and Subtitle</b> DEVELOPMENT AND TESTING OF A NOVEL ANCHOR-PROFILED FRP JACKET SYSTEM FOR EFFECTIVE CONFINEMENT OF RECTANGULAR CONCRETE COLUMNS		<b>5. Report Date</b> February 2025	
		<b>6. Performing Organization Code</b> N/A	
<b>7. Author(s)</b> Bora Genceturk, 0000-0001-6920-0834 Botong Zheng, 0000-0001-7719-1501		<b>8. Performing Organization Report No.</b> PSR-23-04 TO 074	
<b>9. Performing Organization Name and Address</b> METRANS Transportation Center University of Southern California University Park Campus, RGL 216 Los Angeles, CA 90089-0626		<b>10. Work Unit No.</b> N/A	
		<b>11. Contract or Grant No.</b> USDOT Grant 69A3551747109 65A0674	
<b>12. Sponsoring Agency Name and Address</b> U.S. Department of Transportation Office of the Assistant Secretary for Research and Technology 1200 New Jersey Avenue, SE, Washington, DC 20590		<b>13. Type of Report and Period Covered</b> Final report (March 13 2025 – December 31 2024)	
		<b>14. Sponsoring Agency Code</b> USDOT OST-R	
<b>15. Supplementary Notes</b> <a href="https://doi.org/10.25554/fvcc-fs92">https://doi.org/10.25554/fvcc-fs92</a>			
<b>16. Abstract</b> Externally bonded fiber-reinforced polymer (FRP) jacketing has become a widely used technique for strengthening reinforced concrete (RC) columns due to its ease of application. However, its effectiveness is significantly limited when applied to rectangular concrete columns. To address this issue, this research project investigated two potential approaches to enhance the performance of FRP jacketing for rectangular columns: FRP anchoring systems and innovative FRP profiling systems. An experimental program was conducted, involving six groups of columns. The results indicated that the FRP anchoring system provided limited effectiveness, whereas the FRP profiling system showed promising potential, although further experimental validation is needed to confirm its performance. Additionally, a comprehensive database was compiled from the literature, encompassing 24 studies and 406 column tests on square and rectangular columns with FRP confinement relevant to this study. This database will serve as a reference for further analysis of the experimental results.			
<b>17. Key Words</b> Fiber-Reinforced Polymer (FRP), Rectangular Columns, Confinement Effectiveness		<b>18. Distribution Statement</b> No restrictions.	
<b>19. Security Classif. (of this report)</b> Unclassified	<b>20. Security Classif. (of this page)</b> Unclassified	<b>21. No. of Pages</b> 47	<b>22. Price</b> N/A

# Contents

Acknowledgements.....	i
Abstract.....	ii
Executive Summary.....	iii
Introduction .....	1
TASK 1: Design of FRP anchors and profiled FRP jacket system.....	2
FRP anchors.....	2
FRP profiling .....	6
TASK 2: Fabrication and testing of scaled concrete columns with different strengthening configurations .....	8
Column fabrication .....	9
Test setup.....	18
Group 1 results .....	19
Group 2 results .....	22
Group 3 results .....	27
Group 4 results .....	31
Group 5 results .....	35
Group 6 results .....	40
Summary of test results.....	45
TASK 3: Comparative analysis of test data against published data in the literature .....	46
CONCLUSIONS AND RECOMMENDATIONS FOR FUTURE RESEARCH .....	51
Data Management Plan .....	53

## **About the Pacific Southwest Region University Transportation Center**

The Pacific Southwest Region University Transportation Center (UTC) is the Region 9 University Transportation Center funded under the US Department of Transportation's University Transportation Centers Program. Established in 2016, the Pacific Southwest Region UTC (PSR) is led by the University of Southern California and includes seven partners: Long Beach State University; University of California, Davis; University of California, Irvine; University of California, Los Angeles; University of Hawaii; Northern Arizona University; Pima Community College.

The Pacific Southwest Region UTC conducts an integrated, multidisciplinary program of research, education and technology transfer aimed at *improving the mobility of people and goods throughout the region*. Our program is organized around four themes: 1) technology to address transportation problems and improve mobility; 2) improving mobility for vulnerable populations; 3) Improving resilience and protecting the environment; and 4) managing mobility in high growth areas.

### **U.S. Department of Transportation (USDOT) Disclaimer**

The contents of this report reflect the views of the authors, who are responsible for the facts and the accuracy of the information presented herein. This document is disseminated in the interest of information exchange. The report is funded, partially or entirely, by a grant from the U.S. Department of Transportation's University Transportation Centers Program. However, the U.S. Government assumes no liability for the contents or use thereof.

### **California Department of Transportation (CALTRANS) Disclaimer**

The contents of this report reflect the views of the authors, who are responsible for the facts and the accuracy of the information presented herein. This document is disseminated under the sponsorship of the United States Department of Transportation's University Transportation Centers program, in the interest of information exchange. The U.S. Government and the State of California assumes no liability for the contents or use thereof. Nor does the content necessarily reflect the official views or policies of the U.S. Government and the State of California. This report does not constitute a standard, specification, or regulation. This report does not constitute an endorsement by the California Department of Transportation (Caltrans) of any product described herein.

### **Disclosure**

Principal Investigator, Co-Principal Investigators, others, conducted this research titled, "Development and testing of a novel anchor-profiled FRP jacket system for effective confinement of rectangular concrete columns" at Sonny Astani Department of Civil and Environmental

Engineering at the University of Southern California. The research took place from March 13, 2024 to December 31, 2024 and was funded by a grant from the California Department of Transportation in the amount of \$71,274.53. The research was conducted as part of the Pacific Southwest Region University Transportation Center research program.

The research was conducted as part of the Pacific Southwest Region University Transportation Center research program.

## Acknowledgements

The authors would like to acknowledge the financial support provided by the California Department of Transportation. The authors thank to Mr. Fidel Hurtado and Mr. Juan Tuchan Rivas in the Structures and Materials Research Laboratory for their valuable assistance during specimen fabrication. The authors are also grateful for the support from Simpson Strong-Tie, particularly to Dr. Aniket Borwankar and Dr. Mike Lin for their contributions.

## **Abstract**

Externally bonded fiber-reinforced polymer (FRP) jacketing has become a widely used technique for strengthening reinforced concrete (RC) columns due to its ease of application. However, its effectiveness is limited when applied to columns with rectangular cross-sections. To address this issue, this research project investigated two potential approaches to enhance the performance of FRP jacketing for rectangular columns: FRP anchoring and innovative FRP profiling. An experimental program was conducted, involving six groups of columns. The results indicated that the FRP anchoring system provided limited effectiveness, whereas the FRP profiling system showed promising potential, although further experimental validation is needed to confirm its performance. Additionally, a comprehensive database was compiled from the literature, encompassing 24 studies and 406 column tests on square and rectangular columns with FRP confinement relevant to this study. This database will serve as a reference for further analysis of the experimental results.

# DEVELOPMENT AND TESTING OF A NOVEL ANCHOR-PROLFILED FRP JACKET SYSTEM FOR EFFECTIVE CONFINEMENT OF RECTANGULAR CONCRETE COLUMNS

## Executive Summary

This research project investigated the effectiveness of externally bonded fiber-reinforced polymer (FRP) jacketing for strengthening rectangular reinforced concrete (RC) columns, addressing the known limitations of FRP confinement in non-circular geometries. While FRP jacketing is highly effective for circular columns as a result of the uniform confinement, its performance in rectangular columns is hindered by uneven stress distribution and premature FRP rupture at corners.

To enhance the confinement for rectangular columns, two strategies were explored: FRP anchoring and innovative FRP profiling. The experimental program included six groups of scaled concrete columns subjected to uniaxial compression tests. Results indicated that FRP anchoring systems, including both part-through and through-anchor configurations, provided minimal capacity improvement beyond direct FRP jacketing. Similarly, the geofoam profiling system did not yield significant performance gains due to the material's low stiffness, which was insufficient to support the FRP confinement.

Conversely, the steel tube profiling system demonstrated more promising results, with one specimen achieving a 16.6% increase in axial capacity. However, performance variability was observed, primarily due to inconsistencies in FRP jacket installation, such as slack and lack of surface flatness. These findings highlight the critical role of installation quality in achieving confinement effectiveness.

Based on the experimental data, it is recommended that future research focus on developing a hybrid profiling system that combines the flat surface of geofoam with the structural stiffness of steel tubes. A comprehensive experimental program should be designed to evaluate this hybrid system, considering parameters such as support stiffness, profile dimensions, and FRP configurations.

This study provides valuable insights into the limitations and potential improvements of FRP confinement for rectangular RC columns. The proposed hybrid system offers a promising direction for enhancing structural performance, with implications for more effective and reliable retrofitting solutions in structural engineering applications.

## Introduction

Externally bonded fiber-reinforced polymer (FRP) jacketing has become a widely used technique for strengthening reinforced concrete (RC) columns due to its ease of application, often eliminating the need for more labor-intensive methods such as casting additional concrete or installing heavy steel jacketing. While highly effective for circular columns, FRP jacketing is significantly less effective for rectangular concrete columns. This limitation primarily stems from the non-uniform confinement provided by the FRP. In circular columns, confinement is mostly uniform due to mainly tensile stresses being generated in the FRP, producing predictable and enhanced structural performance. In rectangular columns, however, confinement is uneven: the flat sides of the column receive very low confinement, while the corners experience significantly higher confinement. As a result, a large portion of the rectangular column's cross-section remains inadequately confined by the FRP. Additionally, issues arise such as the premature rupture of the FRP around the corners due to high strain concentrations.

To address this issue, this research project explored two potential approaches to improve the effectiveness of FRP jacketing for rectangular columns: FRP anchoring systems and innovative FRP profiling systems. Both methods are designed to enhance confinement along the flat surfaces of the column. These enhancements were evaluated through scaled concrete columns subjected to uniaxial compression testing—a well-established technique for assessing the performance of various confining systems. By examining the results from different groups, the study shed light on the effectiveness of the anchoring and profiling strategies in enhancing the performance of FRP jacketing for rectangular concrete columns.

This project includes four tasks:

Task 1: Design of FRP anchors and profiled FRP jacket system.

Task 2: Fabrication and testing of scaled concrete columns with different strengthening configurations.

Task 3: Comparative analysis of test data against published data in the literature.

Task 4: Preparation of the final report.

This final report provides a comprehensive summary of the details and findings from Tasks 1, 2, and 3.

## TASK 1: Design of FRP anchors and profiled FRP jacket system

In this project, two innovative FRP strengthening strategies were proposed to enhance the confinement of rectangular columns without altering their cross-section. The first strategy involves using FRP anchors to provide additional bond to the flat sides of the rectangular column. These anchors can be either through anchors, which penetrate the entire cross-section of the column, or part-through anchors, which do not fully penetrate the cross-section. The second strategy involves profiling the FRP jacket. This approach utilizes the tensile stress in the FRP to generate a compressive force component on the flat surfaces, thereby confining the concrete more effectively. Two materials were employed for the profiling system: relatively soft geofoam and stiffer steel tubes. The details of the design are explained below.

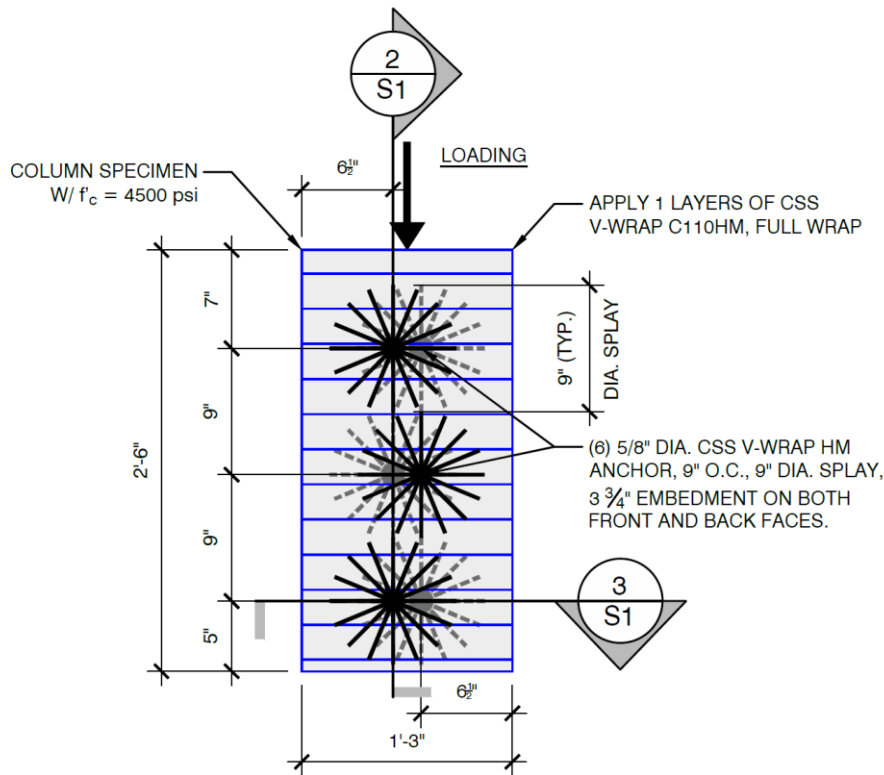
### FRP anchors

The FRP materials used in this project were provided by Simpson Strong-Tie, whose installation team was also responsible for the FRP application under the supervision of the PIs. The same FRP material, Simpson Strong-Tie CSS V-Wrap C 110 HM ([https://www.strongtie.com/unidirectionalcarbon\\_frpfabric/cv-c110hm\\_cssfabric/p/css-v-wrap-c110hm](https://www.strongtie.com/unidirectionalcarbon_frpfabric/cv-c110hm_cssfabric/p/css-v-wrap-c110hm)), was used across all columns. This high-modulus unidirectional carbon fabric has a tensile strength of 670 ksi, a modulus of elasticity of 37,000 ksi, and an elongation at break of 1.65%. After curing, the laminate exhibits a tensile strength of 152 ksi, a modulus of elasticity of 14,700 ksi, and an elongation at break of 1.05%, with a nominal thickness of 0.02 in. All FRP material test data was obtained from the manufacturer, Simpson Strong-Tie, based on their ICC-ES ESR-4930 report. The fabric had a nominal width of 12 in.

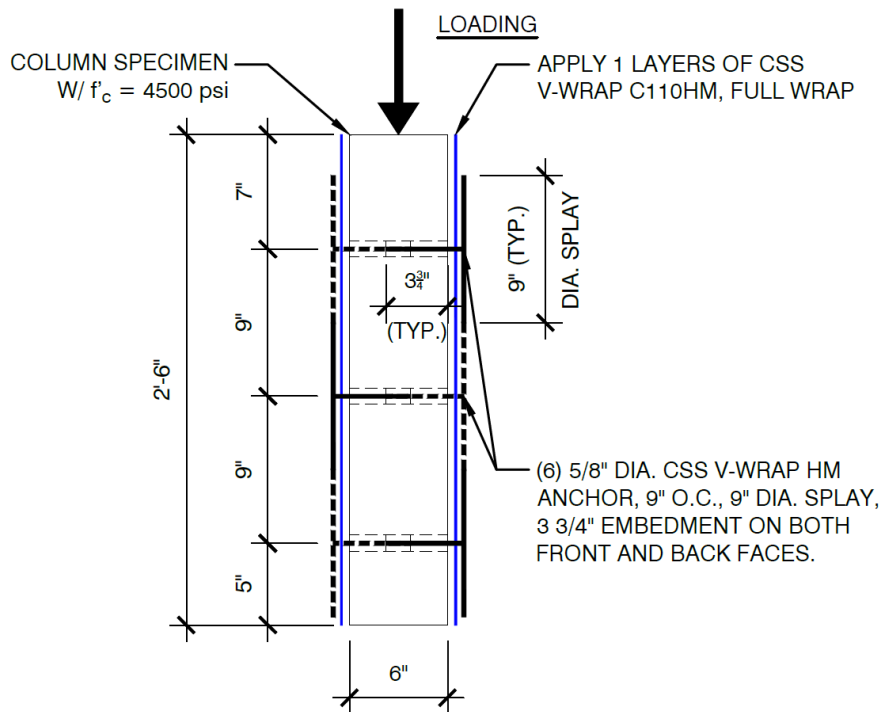
The part-through and through FRP anchoring systems utilized the same type of FRP anchors but different anchor lengths and insertion depths. Simpson Strong-Tie CSS V-Wrap HMCA anchors ([https://www.strongtie.com/anchors\\_fiberreinforcedpolymer/cv-hmca\\_cssfiberanchor/p/css-v-wrap-hmca](https://www.strongtie.com/anchors_fiberreinforcedpolymer/cv-hmca_cssfiberanchor/p/css-v-wrap-hmca)) were used for these systems. These high-strength, high-modulus, unidirectional carbon fiber anchors had a diameter of 0.75 in. The dry fiber has a tensile strength of 790 ksi, a modulus of elasticity of 42,000 ksi, and an elongation at break of 1.9%. After curing, the anchors have a tensile strength of 165 ksi, a modulus of elasticity of 15,000 ksi, and an elongation at break of 1.1%.

As illustrated in Figure 1, the part-through anchoring system incorporated three anchors on each long side of the rectangular columns. The anchor locations were staggered on the opposing sides to ensure that the anchors penetrate only 3.75 in. into the column, which had a width of 6 in. The anchor splay was designed to cover a full 360° with a diameter of approximately 9 in. Anchors were spaced 9 in. apart along the column height, with the total column height measuring 30 in. The through anchoring system shown in Figure 2 incorporated three anchors on each long side of the rectangular columns. The anchor locations on opposing sides were the same as the anchor goes through the column. The anchor splay was designed to cover a full 360° with a diameter of

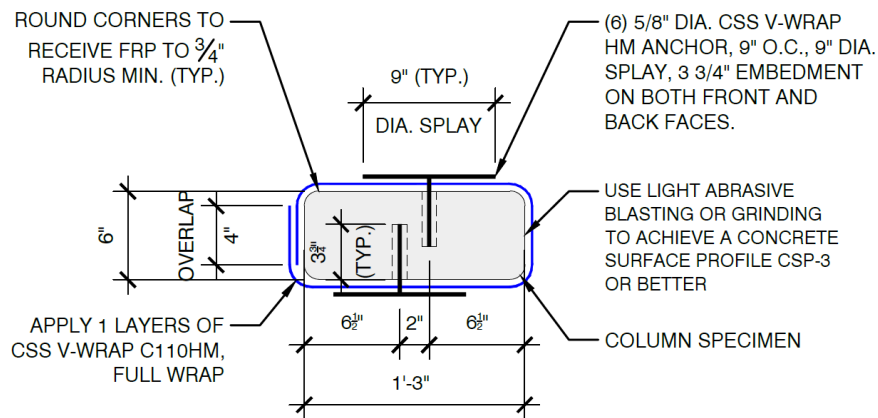
approximately 9 in. Anchors were spaced 9 in. apart along the column height, with the total column height measuring 30 in.



(a) Column elevation view

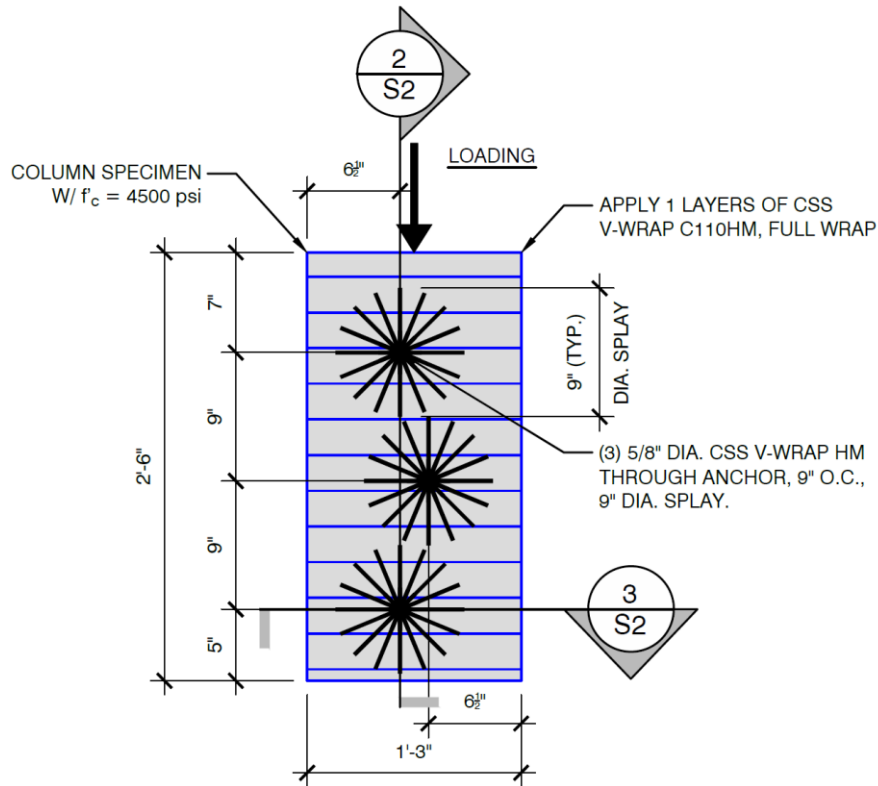


(b) S1/2 vertical cross-section view

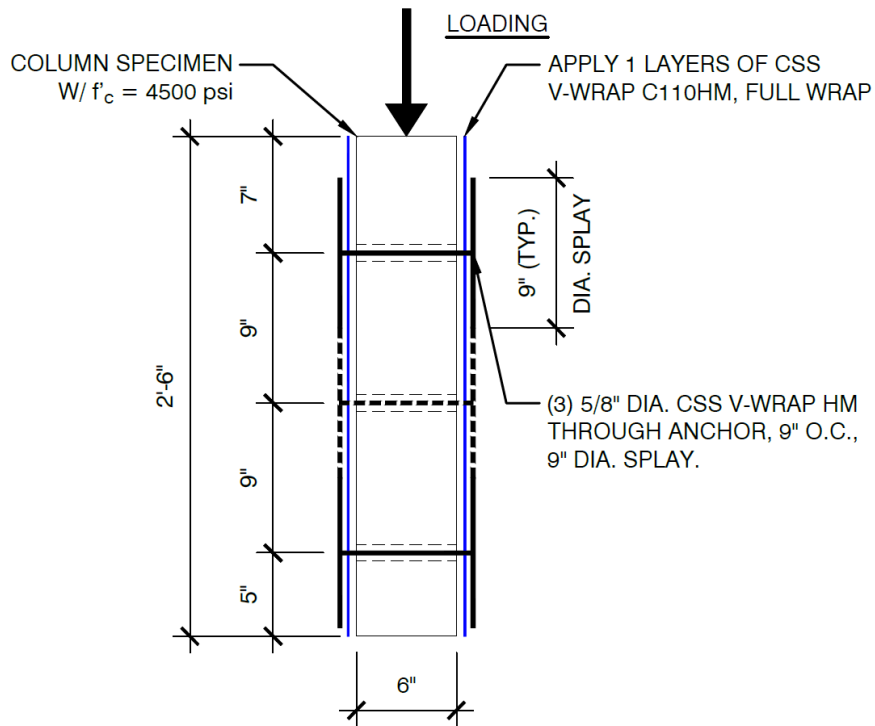


(c) S1/3 horizontal cross-section view

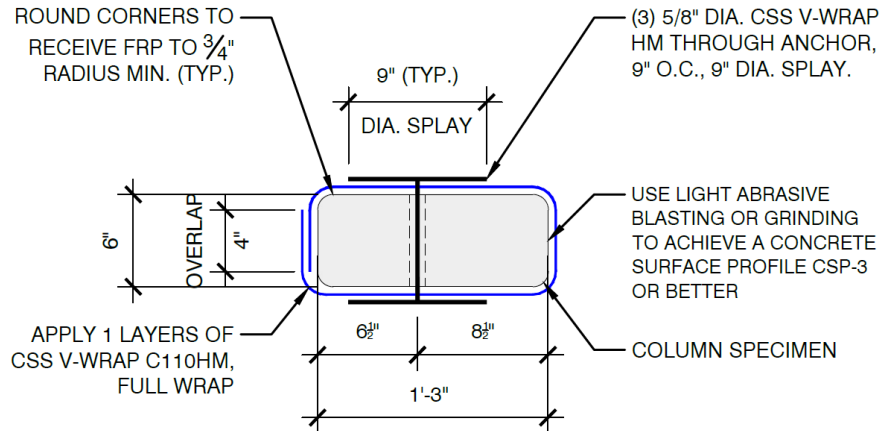
**Figure 1 Part-through FRP anchoring system.**



(a) Column elevation view



(b) S2/2 vertical cross-section view



(c) S2/3 horizontal cross-section view

**Figure 2 Though FRP anchoring system.**

### FRP profiling

The geofoam used in this study was an expanded polystyrene (EPS) with a minimum density of 2.85 lb/ft<sup>3</sup>, a compressive strength of 50 psi, and a modulus of elasticity of 1,860 psi. These properties were provided by the manufacturer. Although its strength and stiffness are significantly lower than those of concrete, EPS geofoam was selected as a filler material to evaluate its potential role in structural confinement. The primary function of the geofoam is to shape the FRP jacket, which ultimately provides the necessary confinement. However, its role extends beyond mere profiling; it must also facilitate the transfer of concrete dilation into tensile forces within the FRP, ensuring that uneven dilation is converted into a more uniform tensile stress distribution. While the inherent mechanical properties of geofoam might suggest limitations, its ability to interact with the FRP confinement system remains an open question. Given its lightweight nature, ease of installation, and potential to influence stress transfer mechanisms, geofoam was considered here a worthwhile investigation as a viable filler material to explore its effectiveness in this application. As shown in Figure 3, the geofoam was machined into a triangular cross-section with a central height of 4.5 in. To ensure a smooth transition and avoid sharp corners at the top vertex of the triangle, a 2-in. radius was introduced, creating a rounded edge where the FRP jacket conforms to the shape. This rounding helps improve the jacket's fit and reduce stress concentrations. The foam length was 28 in., slightly shorter than the 30-in. column. The FRP jacket was wrapped directly around the short side of the concrete column and the surface of the geofoams.

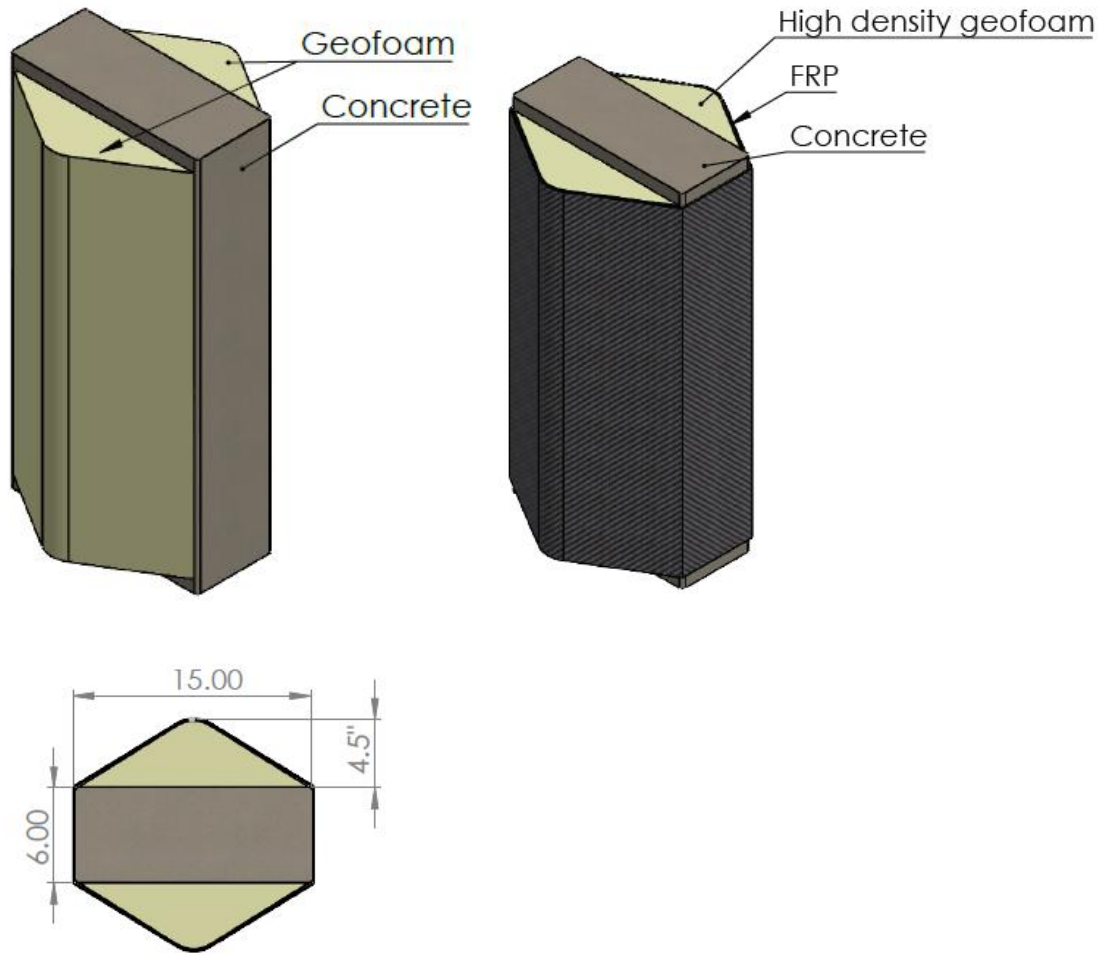


**Figure 3 Geofoam-profiled FRP system.**

The steel tube profilers were made of ASTM A36 steel. As shown in Figure 4, it consisted of a main tube and three legs. The main tube had a 2 in. outer diameter with a 0.25 in. wall thickness, while the three tubular legs featured a 1.25 in. outer diameter and a 0.125 in. wall thickness, spaced 9 in. apart. The legs were welded to the main tube. When installing the supports, two supports were installed on each side of the concrete column, and the FRP jacket was profiled into a trapezoidal shape with a height of 4.5 in.

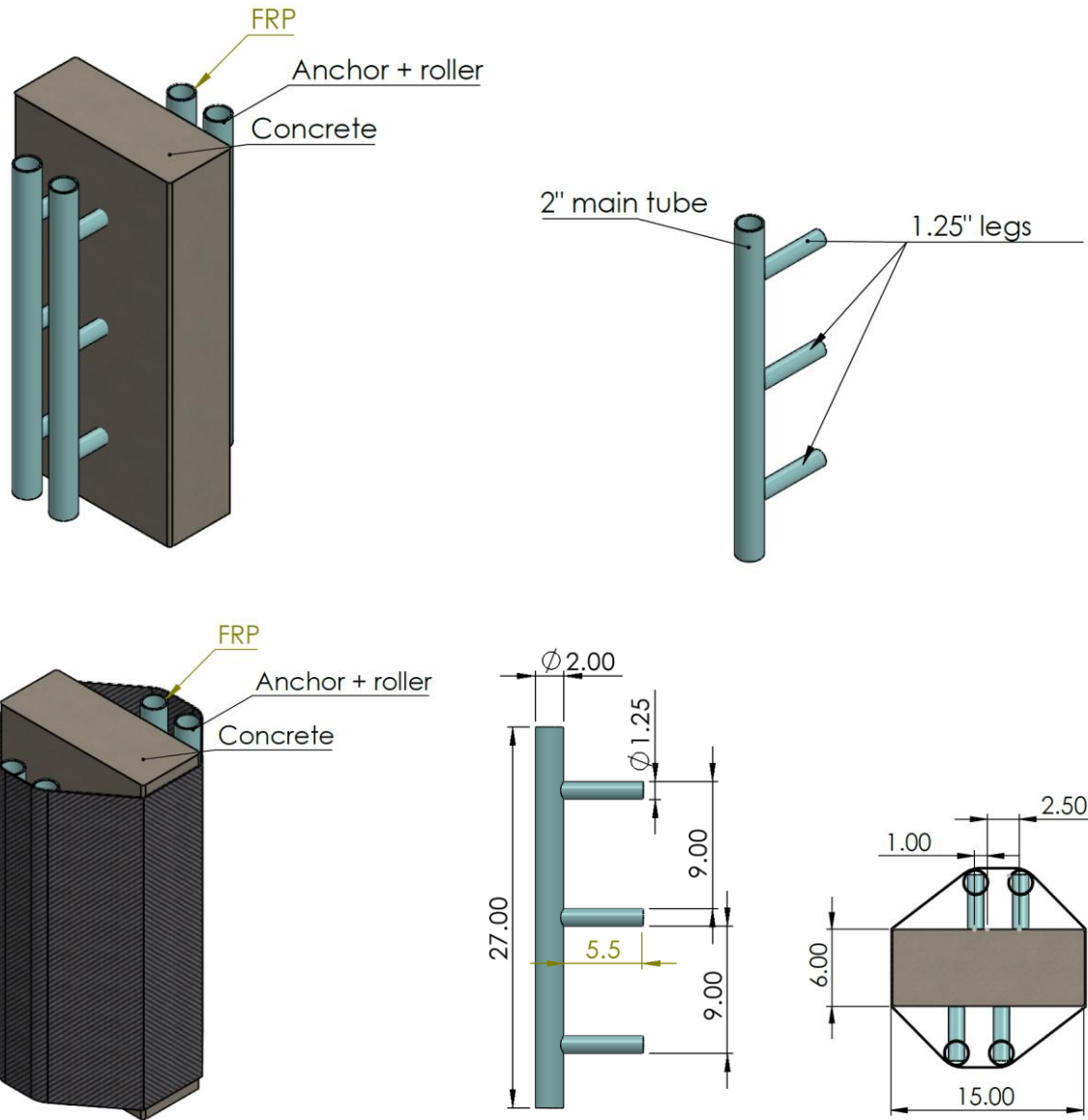


**Figure 4 Steel tube-profiled FRP system.**

## TASK 2: Fabrication and testing of scaled concrete columns with different strengthening configurations

The testing program included six groups, each with two identical columns, totaling 12 scaled concrete columns, as shown in Table 1. Group 1 served as the control group without any confinement. Group 2 used direct FRP jacketing. Groups 3 and 4 involved anchoring systems: Group 3 employed part-through anchors, while Group 4 used through anchors. Groups 5 and 6 focused on profiling methods: Group 5 used geofoam for FRP profiling, and Group 6 used steel tubes for the same purpose. All columns were tested under uniaxial compression until failure.

**Table 1. Test matrix.**

<b>Group</b>	<b>Confinement</b>	<b>Number of columns</b>
1	Control	2
2	Direct FRP	2
3	FRP with part-through anchors	2
4	FRP with through anchors	2
5	FRP with geofoam profiling	2
6	FRP with steel-tube profiling	2

## Column fabrication

All columns had identical dimensions and reinforcement. Each column's cross-section measured 15 in. × 6 in., with an aspect ratio of 2.5, and a height of 30 in., resulting in a height-to-length ratio of 2 and height-to-width ratio of 5. The reinforcement consisted of eight US No. 3 longitudinal rebar, each with a diameter of 0.375 in., and three ties made from the same rebar size. All steel reinforcement is made of Grade 40 steel, with a nominal yield strength of 40 ksi and a yield strain of 0.14%. The ties were spaced at 12 in., with 3 in. left at both the top and bottom of the column. Additionally, a central tie was included in the top and bottom layers of ties, while no tie was used at mid-height. Figure 5 shows the drawings of the rebar cage. Pictures of the rebar cages are shown in Figure 6.

Each rebar cage had eight strain gauges positioned at mid-height. Four gauges were attached to the longitudinal rebar: two on the corner bars, one on the center bar of the short side, and one on the center bar of the long side. Additional four strain gauges were placed on the ties, located at the mid-side positions. Figure 7 shows the locations of the strain gauges.

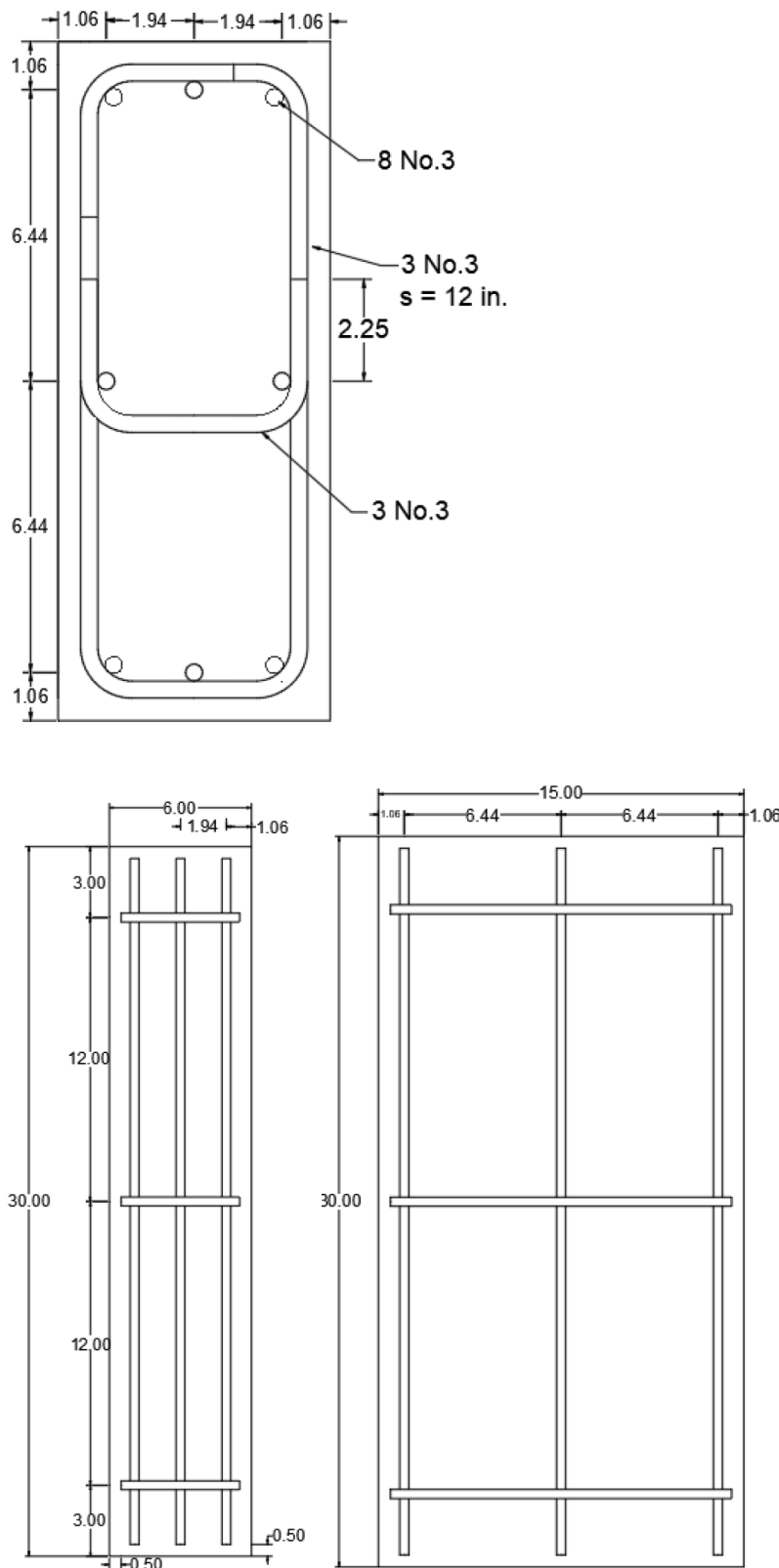


**Figure 5 Rebar cage design**

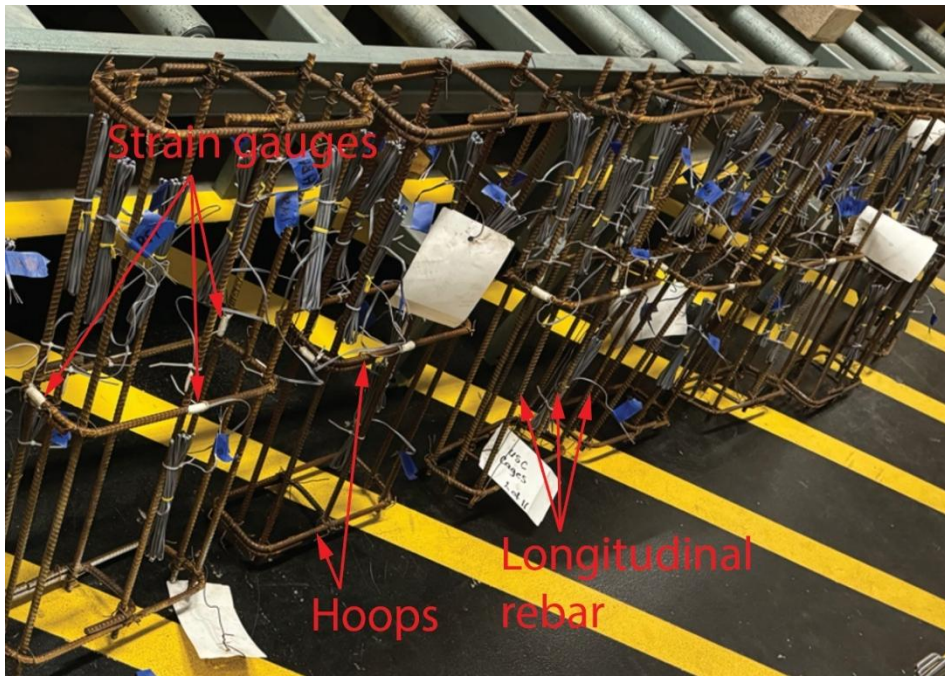


Figure 6 Rebar cages of the scaled columns.

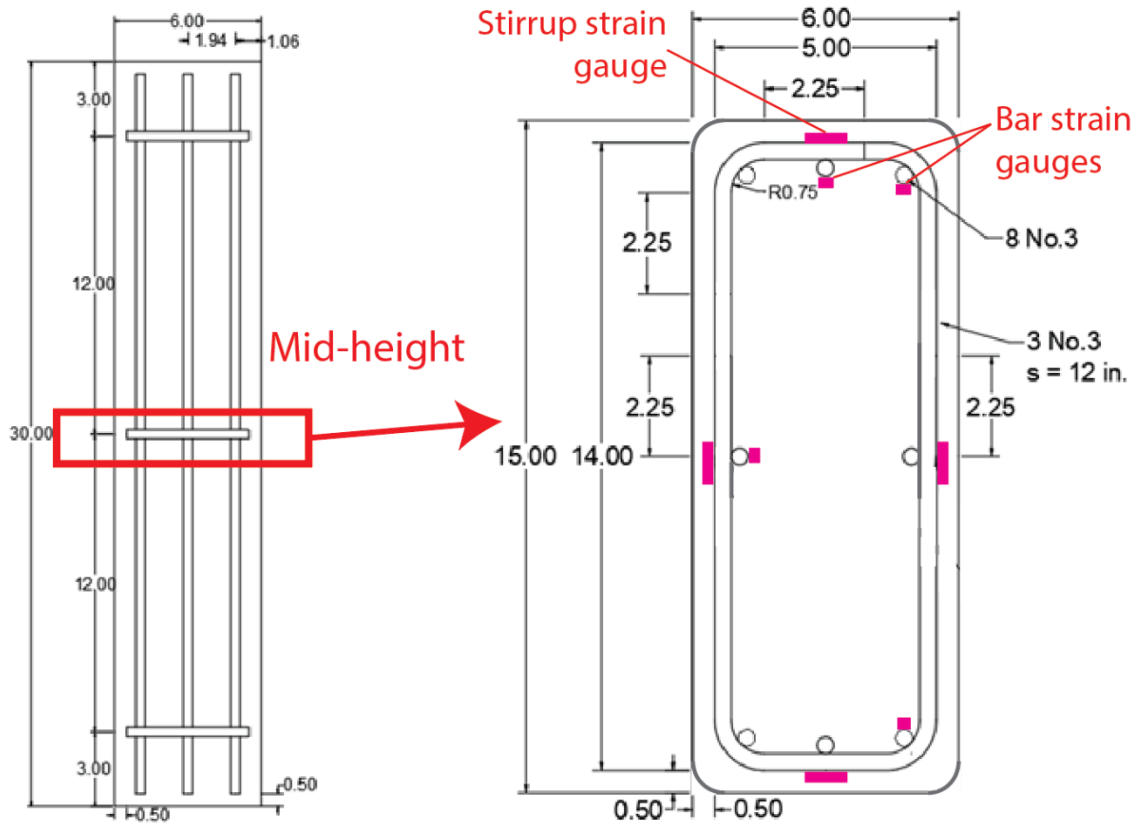
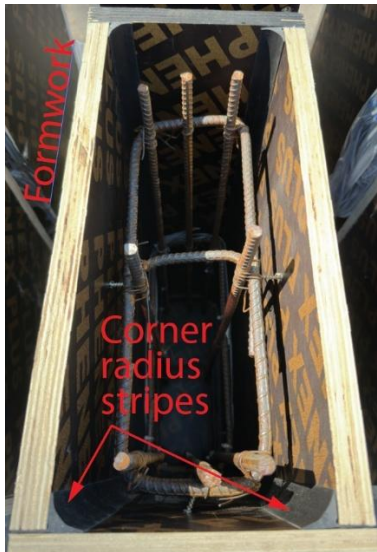


Figure 7 Rebar cage strain gauges.

All columns were cast at the same time using a single batch of concrete, with a design strength of 4,500 psi. The formwork for the columns is shown in Figure 8. To create rounded corners, a Sika chamfer strip with a 0.75-in. radius was applied at the formwork's corners.



**Figure 8 Formwork for columns.**

#### Confinement

The control columns are shown in Figure 9. No further preparation was done for the two control columns.



**Figure 9 Control columns prior to testing.**

For Group 2 FRP confined columns with no anchors, the column surfaces were first primed, and FRP sheets were then applied using a wet layup technique, as illustrated in Figure 10. The fibers were aligned in the circumferential direction of the columns. All columns were reinforced with a single layer of FRP with a 6-in. overlap.



**Figure 10 Priming and wet layup of FRP jacketed columns with no anchors.**

For the Groups 3 and 4 anchoring configurations, anchor holes were first drilled into the columns, followed by priming of the column surfaces. FRP sheets were then applied directly using a wet layup technique. Afterward, holes were cut into the FRP sheets at the locations corresponding to the anchor holes in the columns, as shown in Figure 11. A photograph of the anchor prepared with resin is shown in Figure 12. Next, the prepared FRP anchors were inserted into these holes, as illustrated in Figure 13.



**Figure 11** Drilling anchor holes and wet layup of FRP over the holes.



**Figure 12** Preparing FRP anchor with resin.

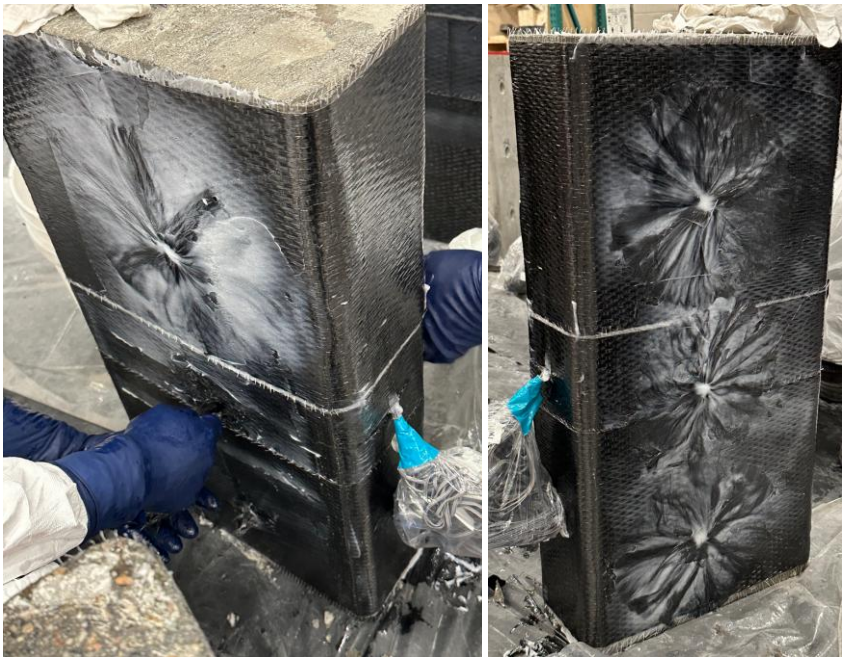


**Figure 13 Inserting FRP anchors.**

For Group 5 geofoam-profiling configuration, the column surface was first primed in the same manner as that for Group 2 columns. Geofoam was then placed on both sides of the column, as illustrated in Figure 14. After priming the geofoam surface, FRP sheets were wrapped around the column short sides and the geofoam surface using a wet layup technique, as shown in Figure 14. The length of the FRP sheet allowed for a 6 in. overlap. The final geofoam-profiled column is shown in Figure 15.



**Figure 14 Preparing geofoam-profiled FRP jacket.**



**Figure 15 Columns with geofoam-profiled FRP jacket.**

For Group 6 steel tube-profiled columns, individual steel tube supports were fabricated, as illustrated in Figure 16. Prior to installation, 2.125 in. diameter holes were drilled into the concrete columns, spaced 9 in. apart (see Figure 16). After the holes were drilled, the column surface was primed, and the holes were filled with structural adhesive, as shown in Figure 17. The tubes were then inserted into the holes. Two tubes were installed on each side of the column to shape the FRP jacket. Once inserted, the legs extended 4.5 in. above the concrete surface, matching the height of the geofoam configuration. Next, the tubes were primed, as shown in Figure 18. Finally, an FRP sheet was wrapped directly around the column on the short side and over the tube supports, as seen in Figure 18.

In addition to the eight rebar strain gauges, two strain gauges were also installed on the surface of the FRP jacket in the hoop direction for all columns except for the control columns. The strain gauge locations are shown in Figure 19.



**Figure 16 Steel-tube and preparation of columns.**



**Figure 17 Installation of tubes on columns.**



**Figure 18 Wrapping of FRP sheets on the steel tubes and concrete.**

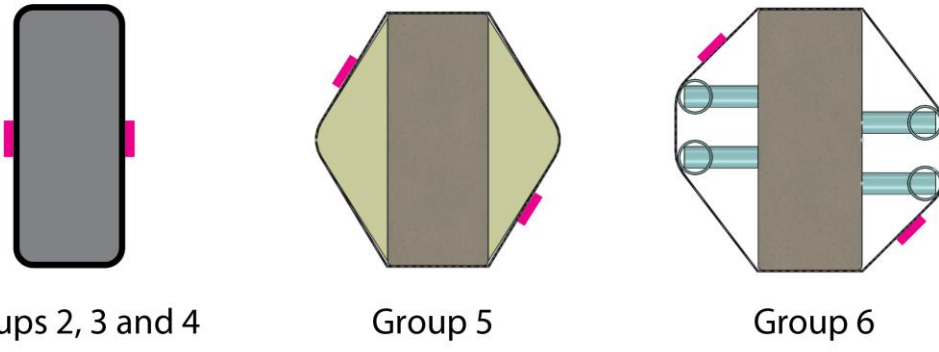


**Figure 19 Strain gauge locations on the FRP jacket.**

## Test setup

The test setup is illustrated in Figure 20. All columns were tested in a hydraulic loading frame with a 600-kip capacity. Each column's base was placed directly on the loading frame, while the top was fitted with a leveling sandwich plate to ensure uniform compression distribution and prevent local concrete damage. Above the sandwich plate, a 1-in.-thick steel plate was positioned to cover the entire cross-section. The loading frame had a spherical loading platen that allowed for 360 degrees swivel for axial load application.

The applied compression load was recorded using the load cell integrated into the loading frame, which also had a 600-kip capacity. Column displacement under compression was measured with a spring-loaded string potentiometer. To set up the potentiometer, a wooden block was bonded to the top of the column, and a wooden base was fixed to the bottom of the loading frame. The string potentiometer was anchored between the wooden block and the base, measuring the column's shortening over 27 in. The strain gauges were directly connected to the data acquisition system, which also captured data from the load cell and the string potentiometer.

Displacement-controlled monotonic loading was applied on all columns, the loading rate was 0.01 in./min., all columns were loaded to failure.

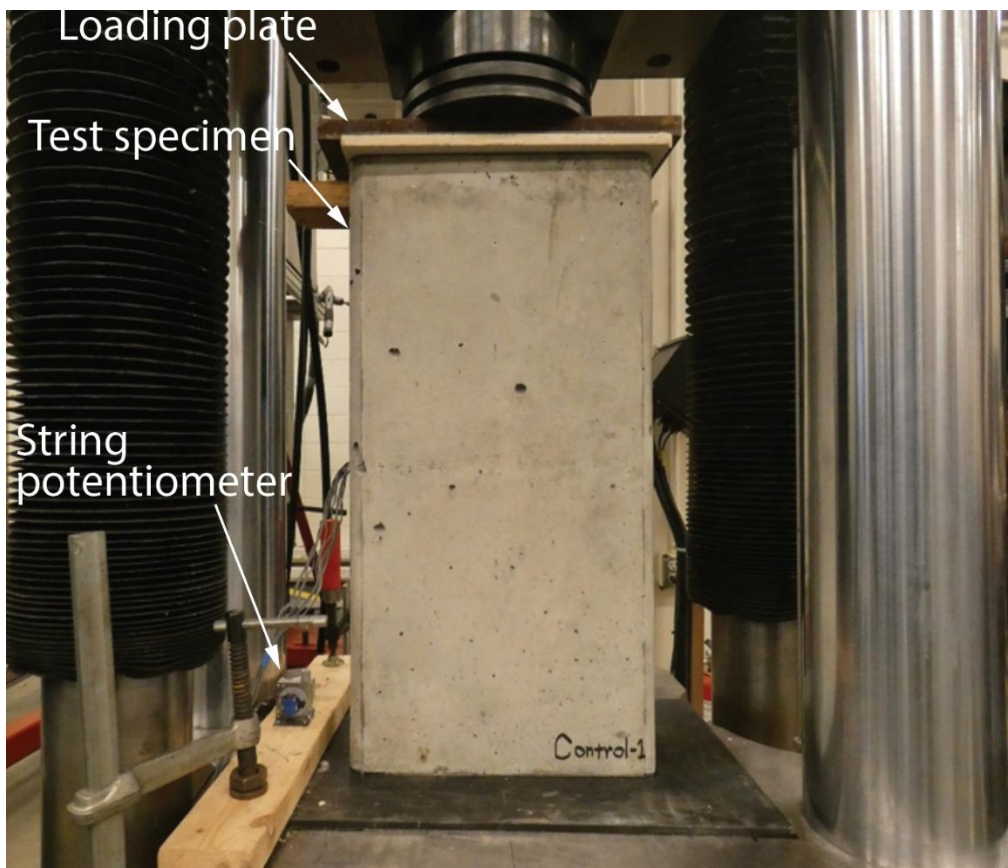


**Figure 20** Test setup.

## Group 1 results

The failure of the two control columns is shown in Figure 21. Both columns exhibited concrete crushing failure, characterized by an inclined fracture surface running through the column. The load versus shortening curves for the control columns, presented in Figure 22, reveal a nearly linear loading phase that continued up to the peak load. At this point, a sudden drop in load occurred, corresponding to the concrete crushing failure.



**Figure 21 Failure mode of control columns.**

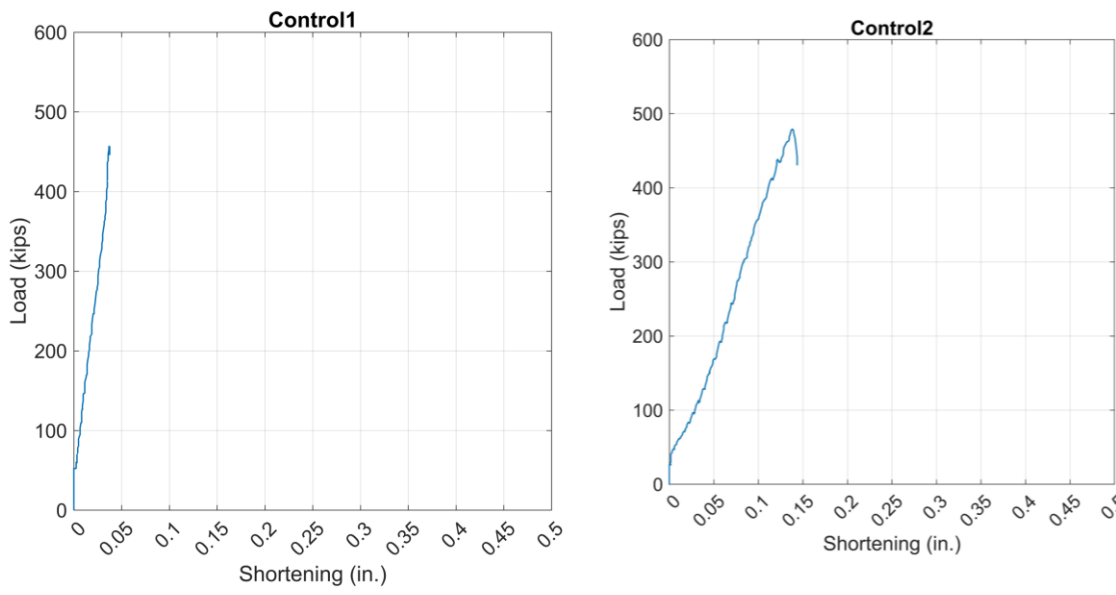


**Figure 22 Axial load versus axial shortening curves for control columns.**

The rebar strain data for the control columns is presented in Figure 23 and Figure 24. The strain data for the longitudinal rebar showed that yielding did not occur up to the point of column

failure. The hoop strain measurements indicate that the ties yielded at the mid-point location along the long side of the column, while no obvious yielding occurred along the short side.

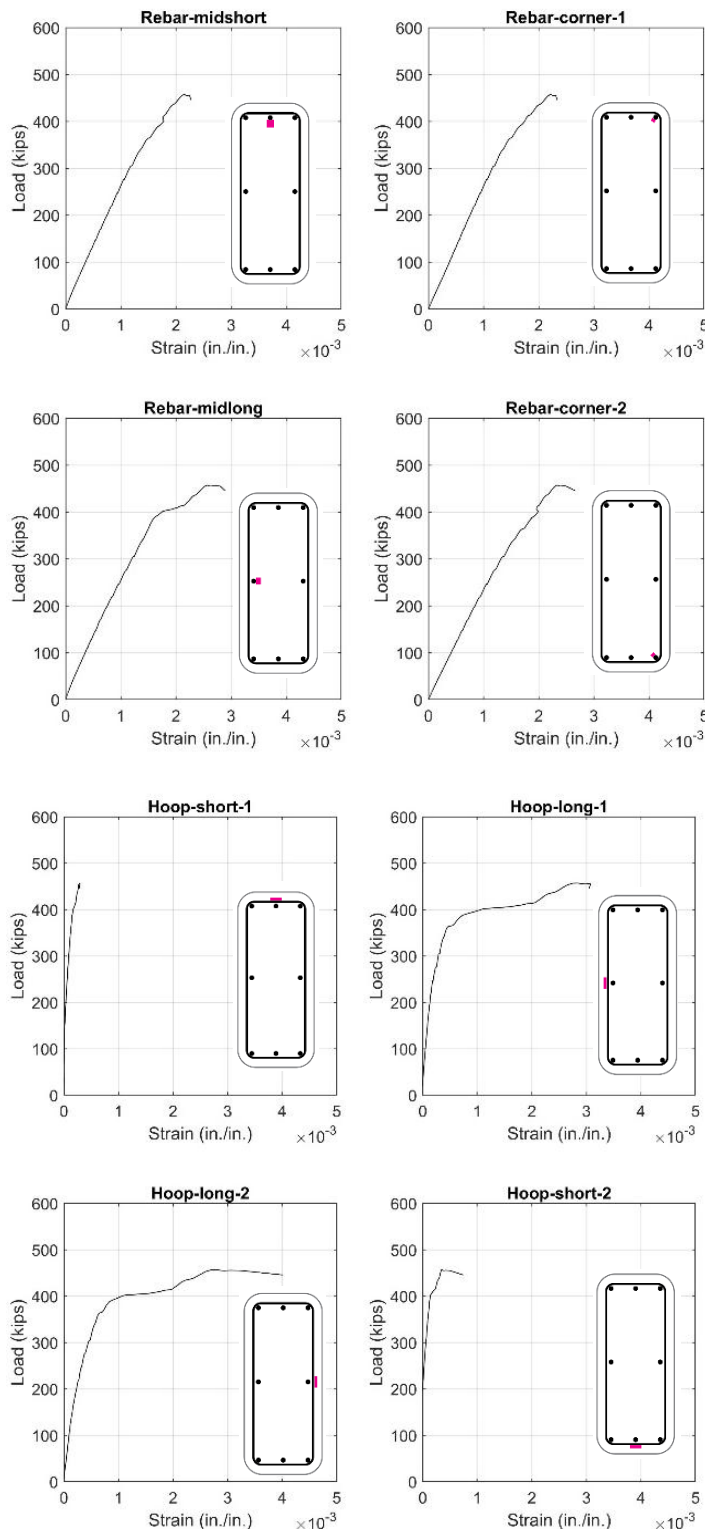


**Figure 23 Rebar strains for control column 1.**

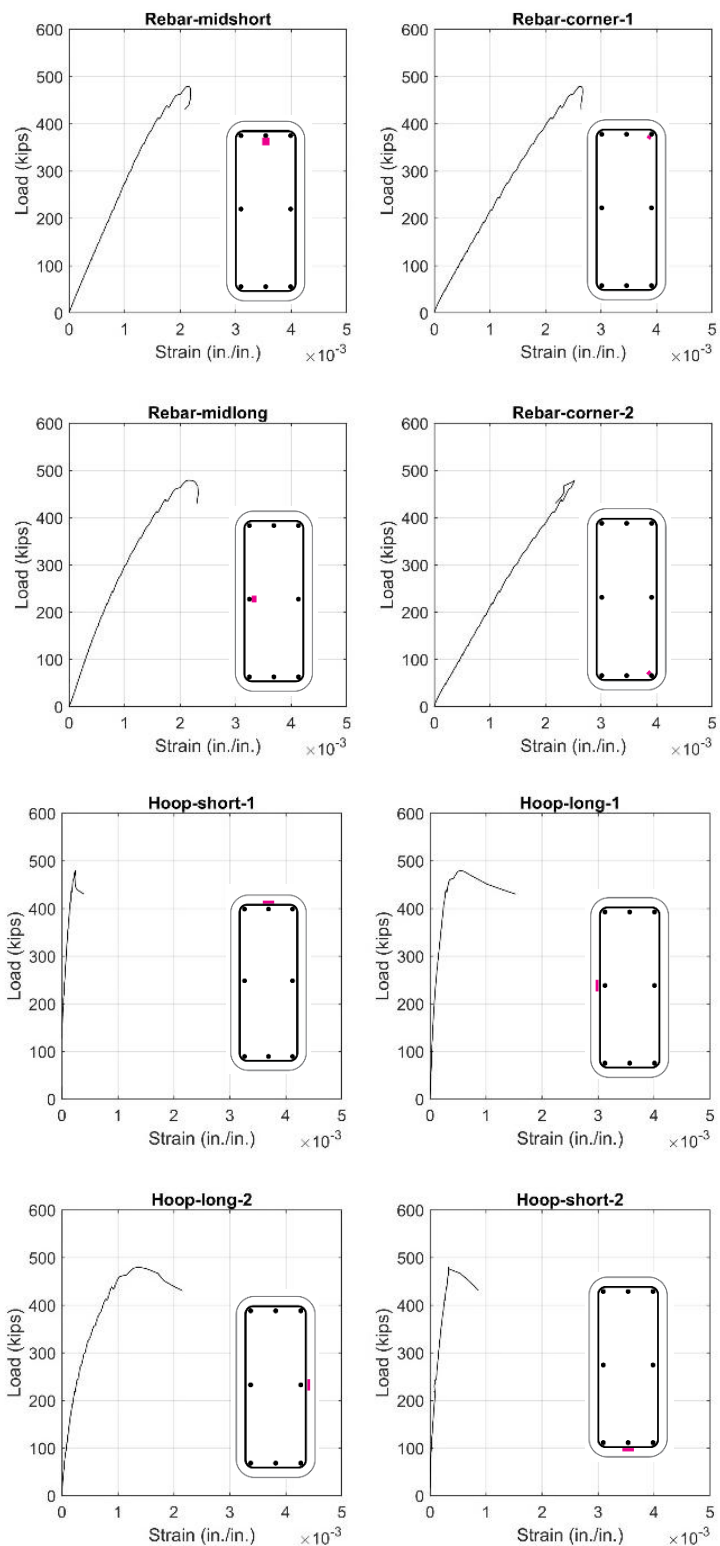
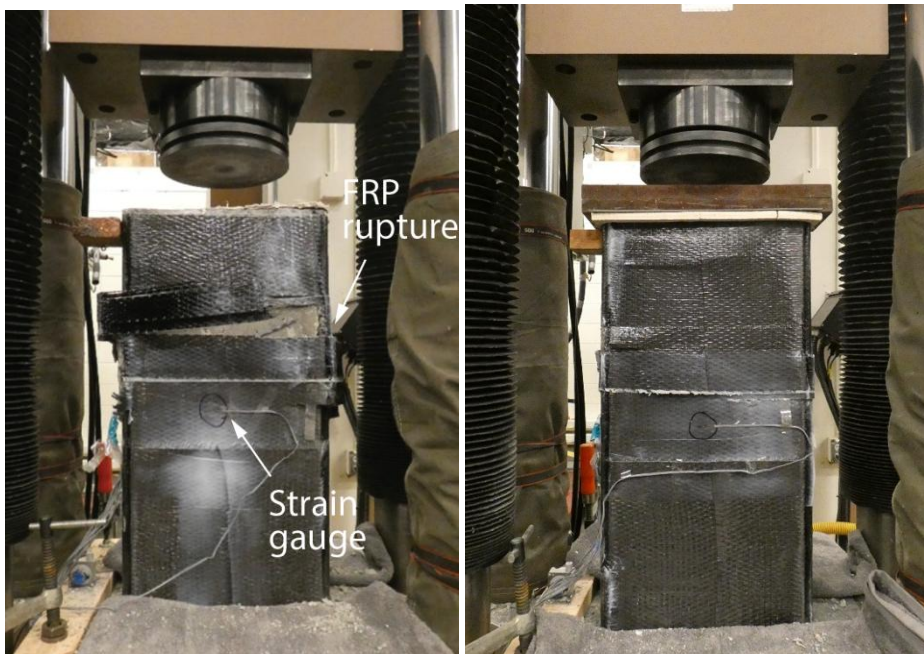


**Figure 24 Rebar strains for control column 2.**

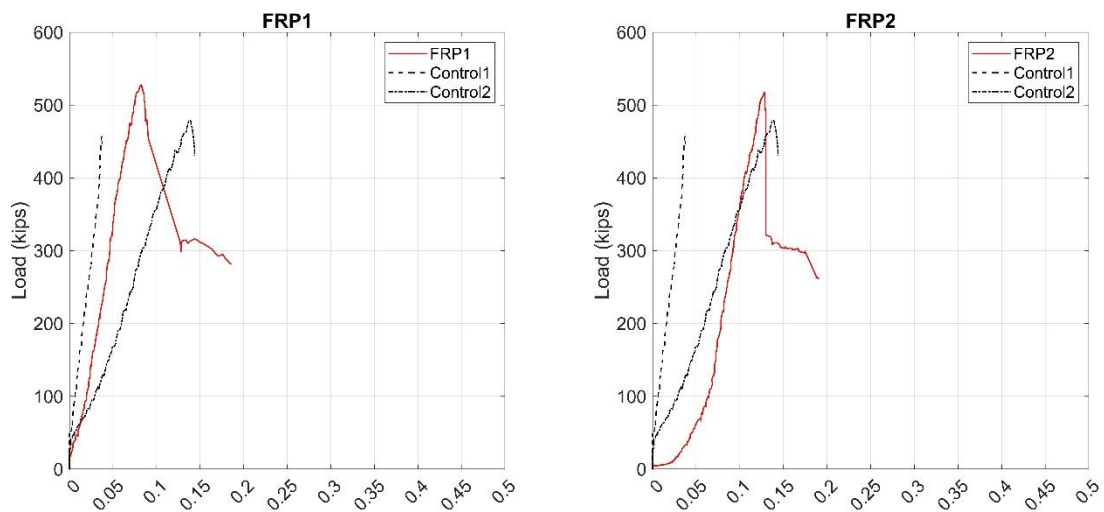
## Group 2 results

The failure of the Group 2 columns is illustrated in Figure 25. Both columns exhibited a similar failure. Upon reaching the peak load, concrete crushing occurred with an audible noise, followed by a sudden drop in load. However, the columns were able to continue carrying load with no immediate FRP rupture. With continued loading and shortening, significant dilation of the concrete was observed, accompanied by cracking noises from the FRP jacket. Eventually, FRP rupture occurred at the corners, as shown in Figure 25, leading to complete failure.

The load-shortening curves for the Group 2 columns are presented in Figure 26, along with the curves for the control columns for comparison. After the initial load drop, the Group 2 columns demonstrated a higher deformation capacity compared to the control columns, attributed to the confinement provided by the FRP jacket. However, the sharp drop indicates that the FRP confinement was insufficient to provide a ductile enough second loading branch. Furthermore, both Group 2 columns exhibited an increase in peak load compared to the control columns.

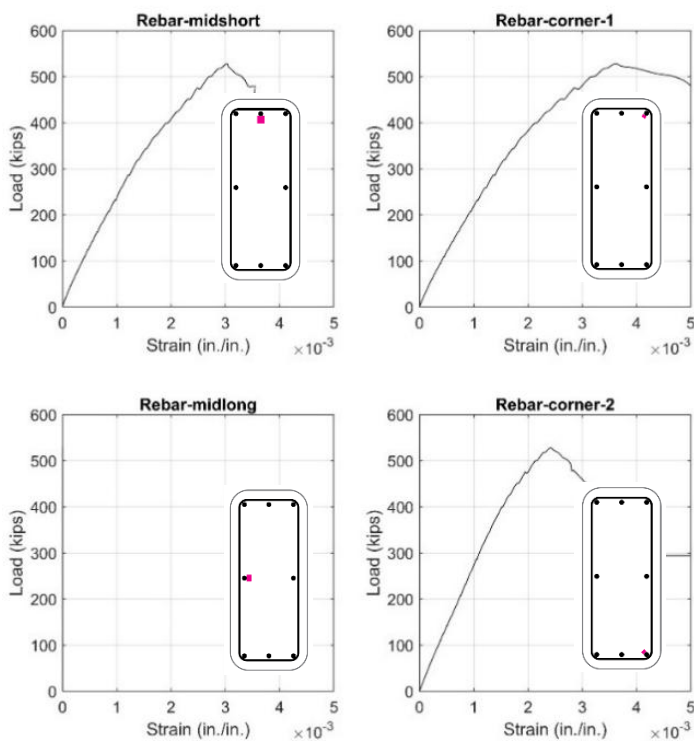


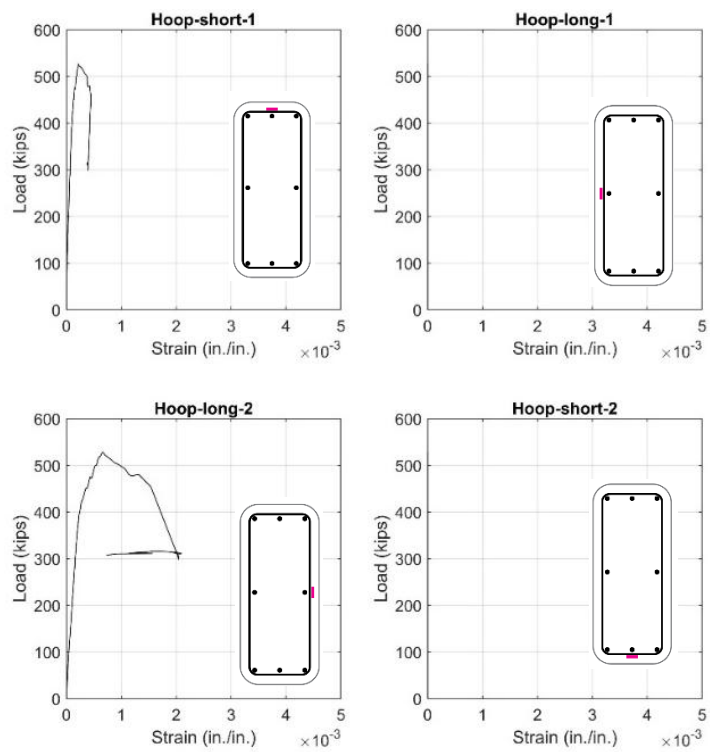
**Figure 25 Failure mode of Group 2 columns.**



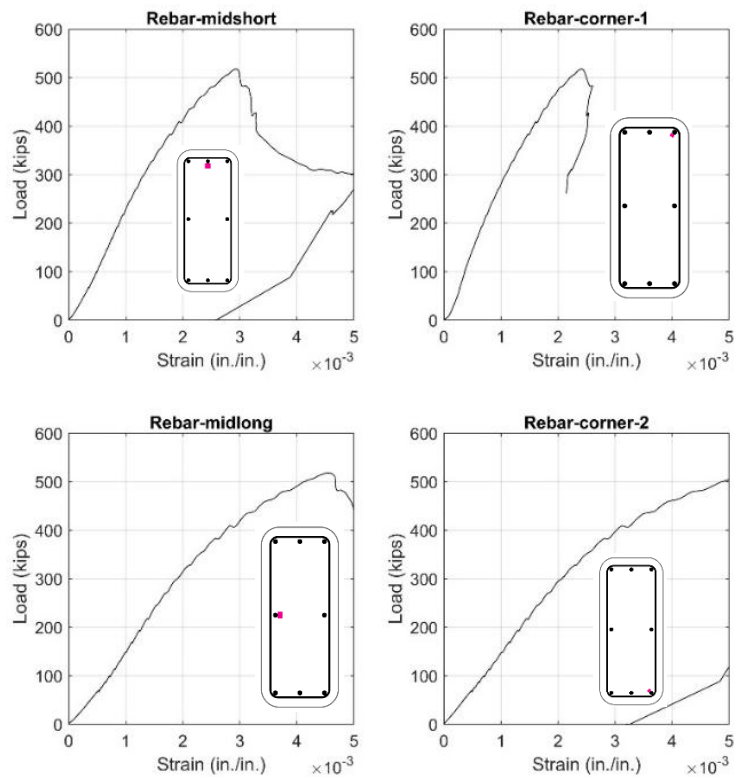
**Figure 26 Axial load versus axial shortening curves for Group 2 columns.**

The rebar strain data for the Group 2 columns are shown in Figure 27 and Figure 28. In Figure 27, the strain gauges at Hoop-long-1, Hoop-short-2, and Rebar-midlong did not record any data, likely due to damage to the gauge or wires during concrete casting. In both columns, yielding of the longitudinal rebar was observed after the peak load, which is attributed to the increased column shortening facilitated by the FRP jacket. The hoop strain measurements reveal that the ties yielded at the mid-point locations along both the long and short sides of the column.





**Figure 27 Rebar strains for Group 2 Column 1.**



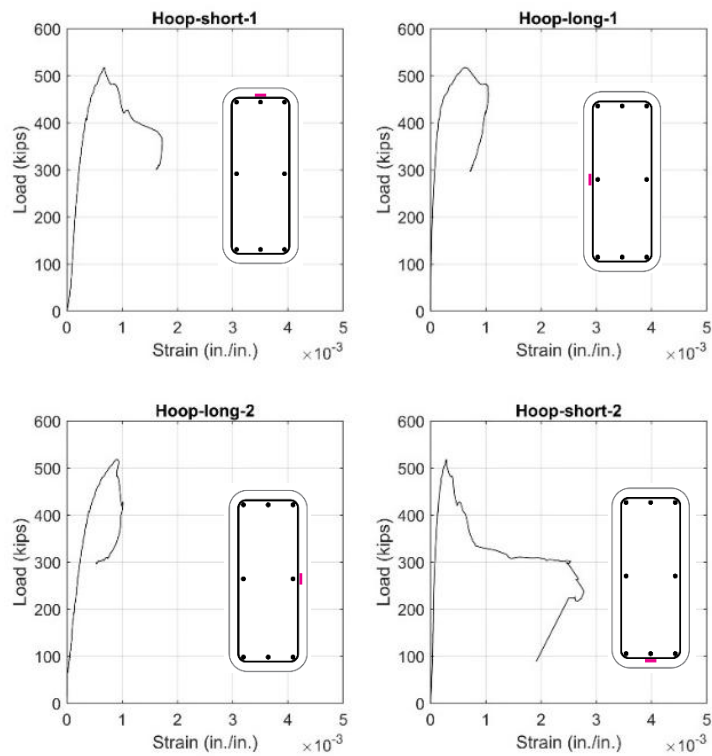
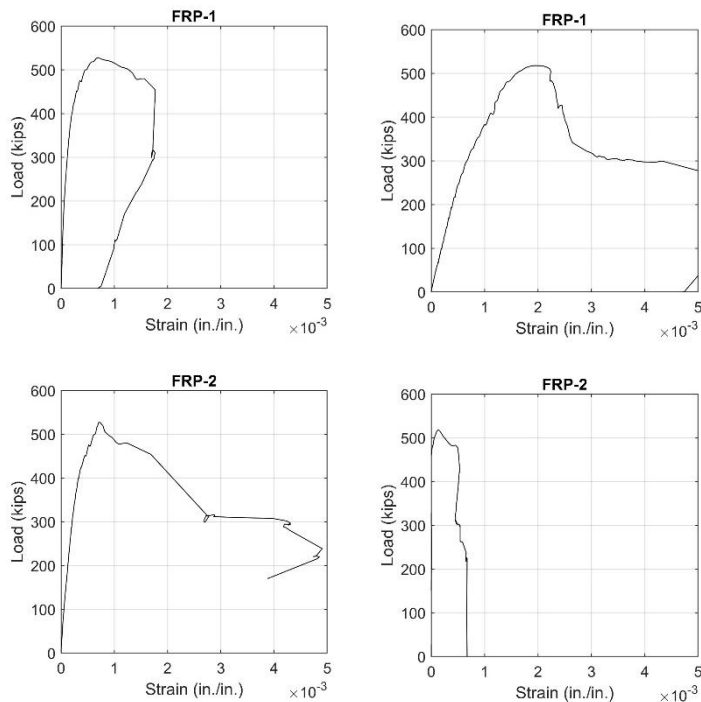


**Figure 28 Rebar strains for Group 2 Column 2.**

The strains measured by the strain gauges bonded to the surface of the FRP jacket are presented in Figure 29. It is seen that for each column, on one side of the column, the FRP strain reached over 0.004 prior to FRP rupture.



(a) Column 1

(b) Column 2

**Figure 29 FRP strains for Group 2 columns.**

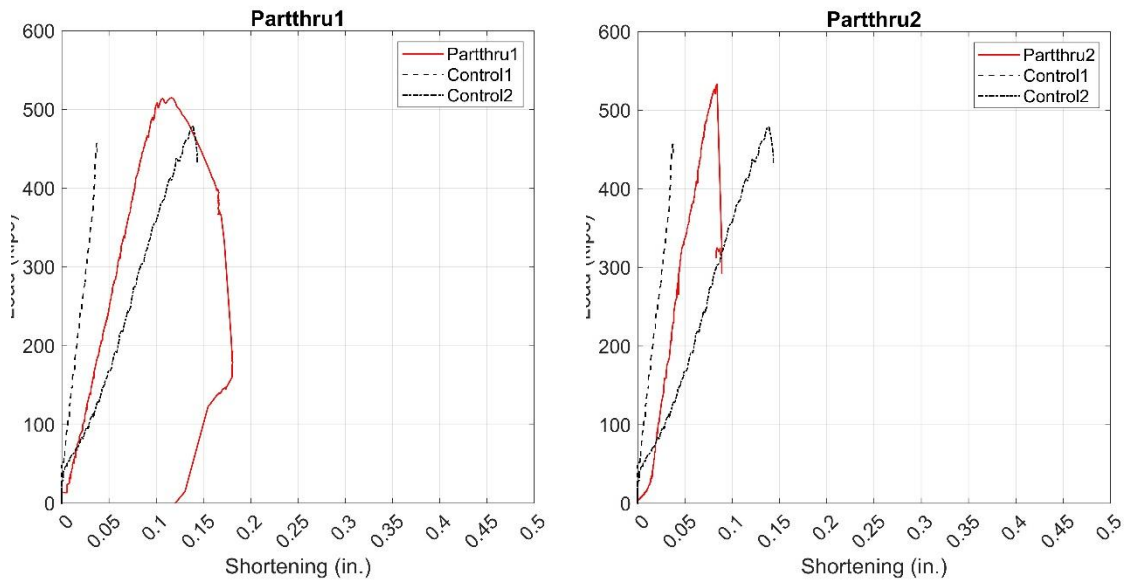
### Group 3 results

The failure process of the Group 3 columns is shown in Figure 30. Both specimens exhibited failure behavior similar to that of the Group 2 columns. At peak load, concrete crushing occurred with an audible noise, followed by a sudden drop in load. However, unlike the Group 2 columns, the FRP rupture occurred at the corners shortly after the load drop, as shown in Figure 30, resulting in complete failure. The load drop stage for Group 3 columns was shorter than that observed for the Group 2 columns.

The load-shortening curves for Group 3 columns are presented in Figure 31, alongside the curves for the control columns for comparison. After the initial load drop, Group 3 columns exhibited a sharp decline, indicating that the FRP confinement was insufficient to provide a ductile second-branch. Nevertheless, both Group 3 columns showed an increase in the peak load compared to the control specimens.

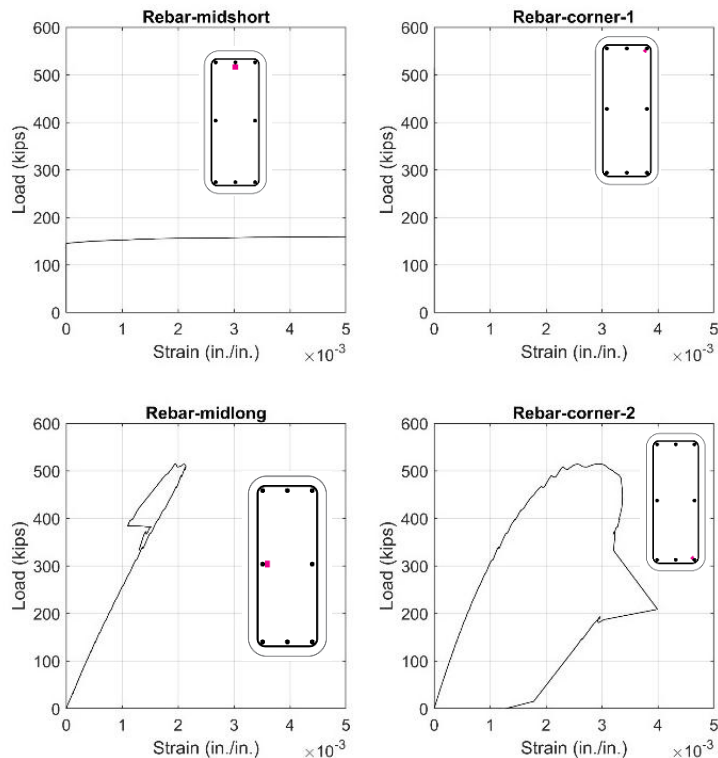


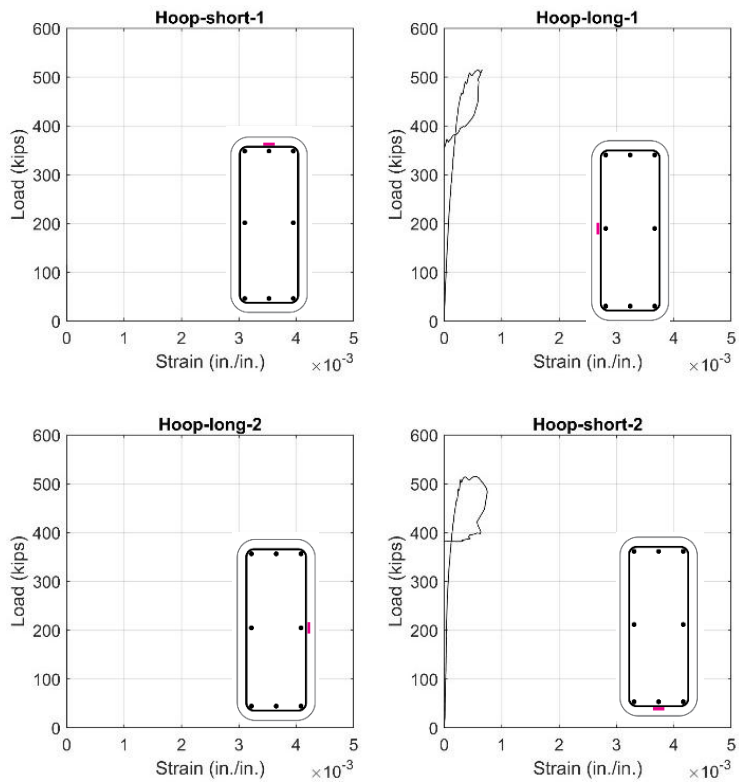
**Figure 30 Failure mode of Group 3 columns.**



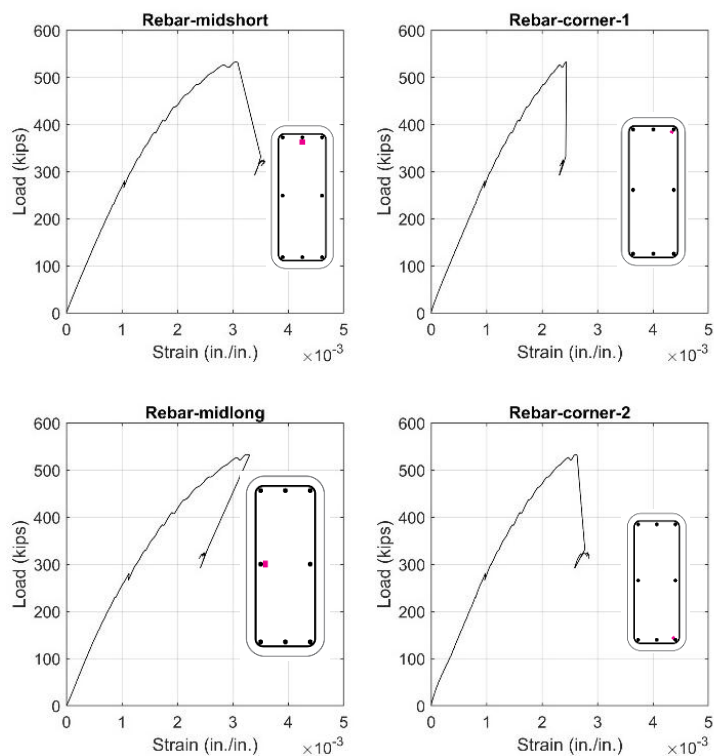
**Figure 31 Axial load versus axial shortening curves for Group 3 columns.**

The rebar strain data for Group 3 columns are presented in Figure 32 and Figure 33. In Figure 32, the strain gauges at Rebar-corner-1, Hoop-short-1, and Hoop-long-2 did not record any data, likely due to damage during concrete casting. The longitudinal rebar strain measurements indicate minimal yielding, attributed to the relatively rapid FRP rupture upon reaching the peak load. Similarly, the hoop strain measurements show no significant evidence of tie yielding.





**Figure 32 Rebar strains for Group 3 Column 1.**



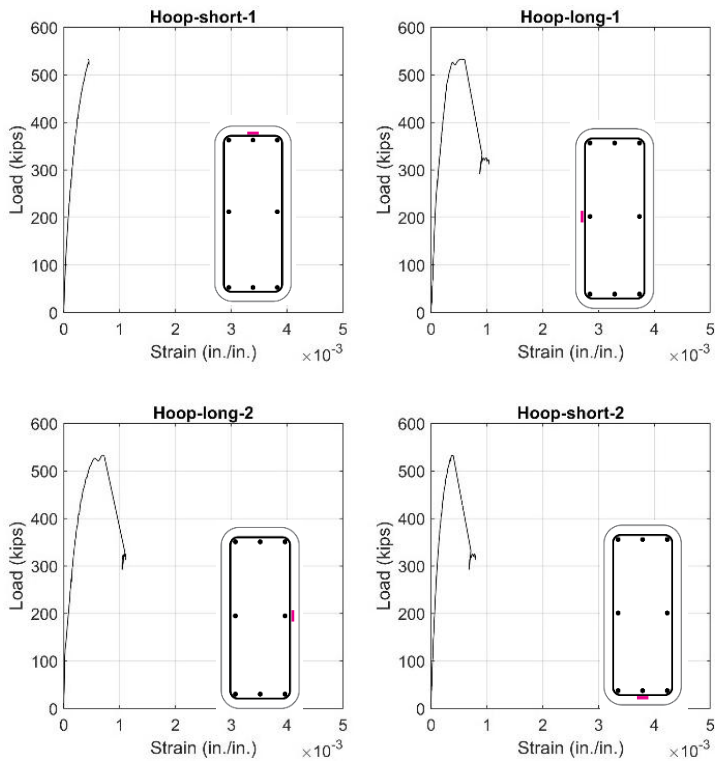


**Figure 33 Rebar strains for Group 3 Column 2.**

The FRP strains are shown in Figure 34. For Column 1, the FRP strain on one side (FRP-2 as shown in Figure 34) of the column exceeded 0.002 before the final rupture. In contrast, Column 2 exhibited no significant increase in FRP strain after reaching the peak load. This suggests that the FRP did not effectively engage in confining the concrete beyond the peak load. Instead, the FRP confinement primarily increased the capacity of the column. A comparison with the FRP strains of Group 2 column shown in Figure 29 suggests that part-through anchors may not enhance the FRP confinement.

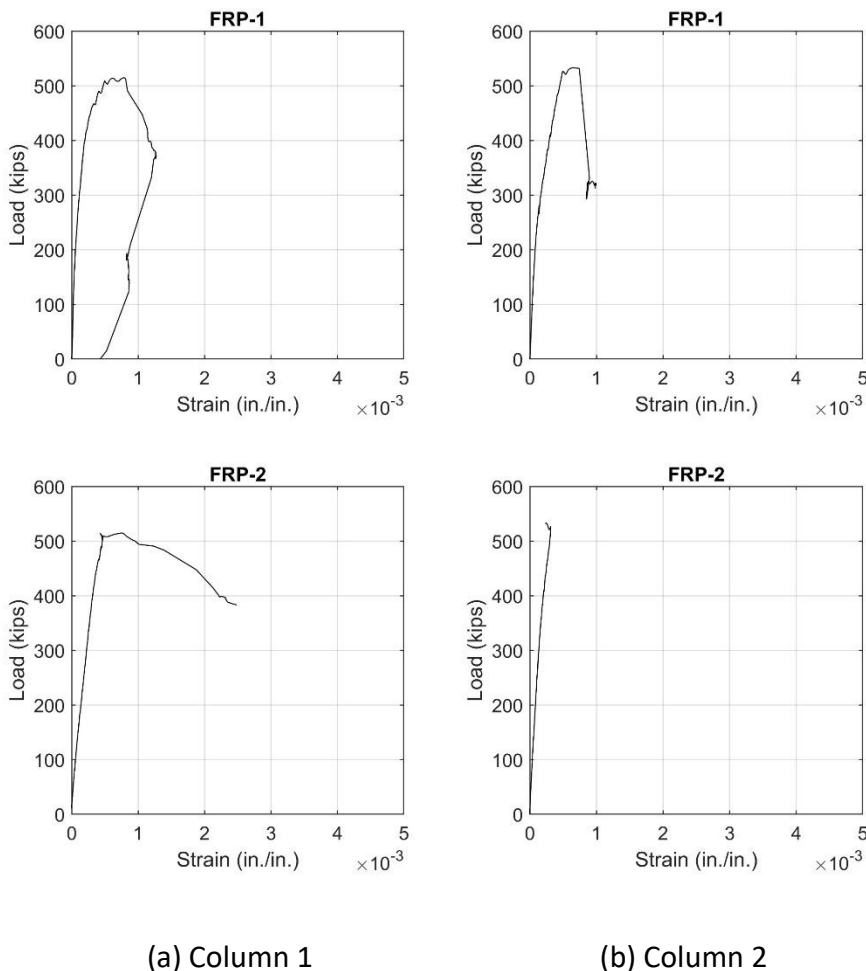


**Figure 34 FRP strains for Group 3 columns.**

## Group 4 results

The failure of Group 4 columns is illustrated in Figure 35. Both columns in Group 4 exhibited a failure similar to that of the Group 2 columns. At peak load, concrete crushing occurred with an audible noise, followed by a sudden drop in the load. FRP rupture did not occur immediately, allowing the columns to continue carrying load as shortening occurred. Eventually, FRP rupture occurred at the corners, as shown in Figure 35, leading to failure.

The axial load versus axial shortening curves for Group 4 columns are presented in Figure 36, alongside the curves for the control columns for comparison. Following the initial load drop, the Group 4 columns displayed a sharp decline; however, the magnitude of the load drop was smaller compared to Groups 2 and 3. While Group 2 and 3 columns experienced a load drop from the peak load to approximately 300 kips, the Group 4 columns dropped to around 400 kips. This suggests that the FRP provided a greater confinement to the concrete upon initial crushing, though it remained insufficient to enable a smooth transition to a secondary loading branch.

Additionally, Column 1 in Group 4 showed no significant increase in peak load, while Column 2 showed a slight improvement.

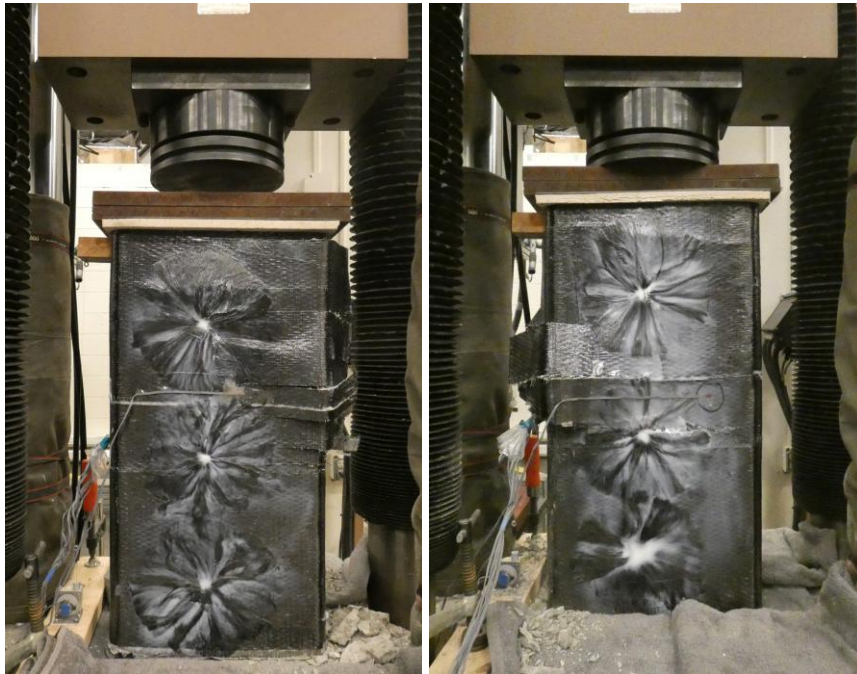


**Figure 35 Failure mode of Group 4 columns.**

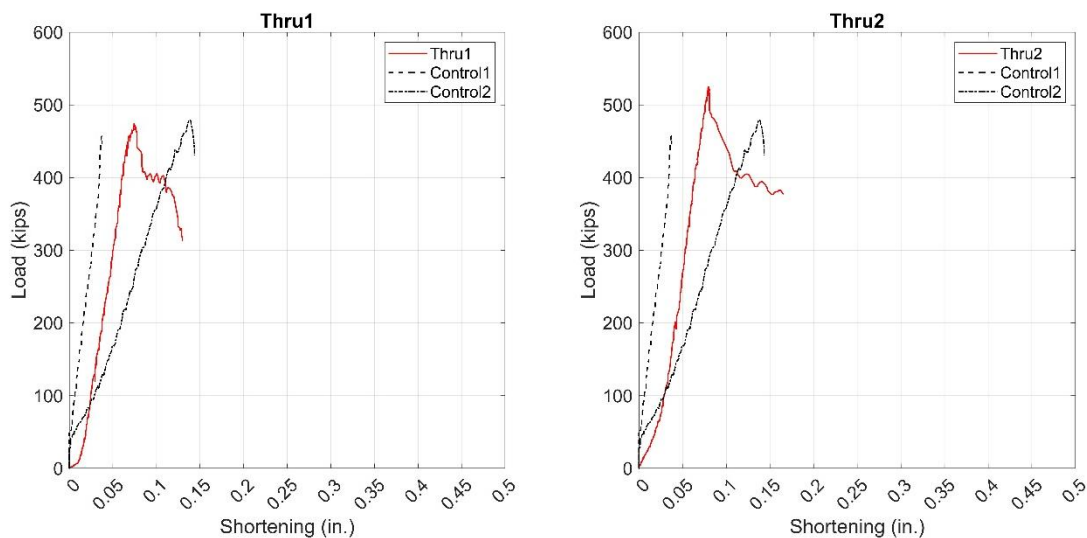


**Figure 36 Axial load versus axial shortening curves for Group 4 columns.**

The rebar strain data for Group 4 columns are presented in Figure 37 and Figure 38. In Figure 37, the strain gauges at Rebar-midshort, Rebar-corner-1, Hoop-short-1, Rebar-midlong, and Hoop-long-2 did not record any data, likely due to damage during concrete casting. The longitudinal

rebar strain measurements indicate minimal yielding. Similarly, the hoop strain measurements show no evidence of tie yielding.

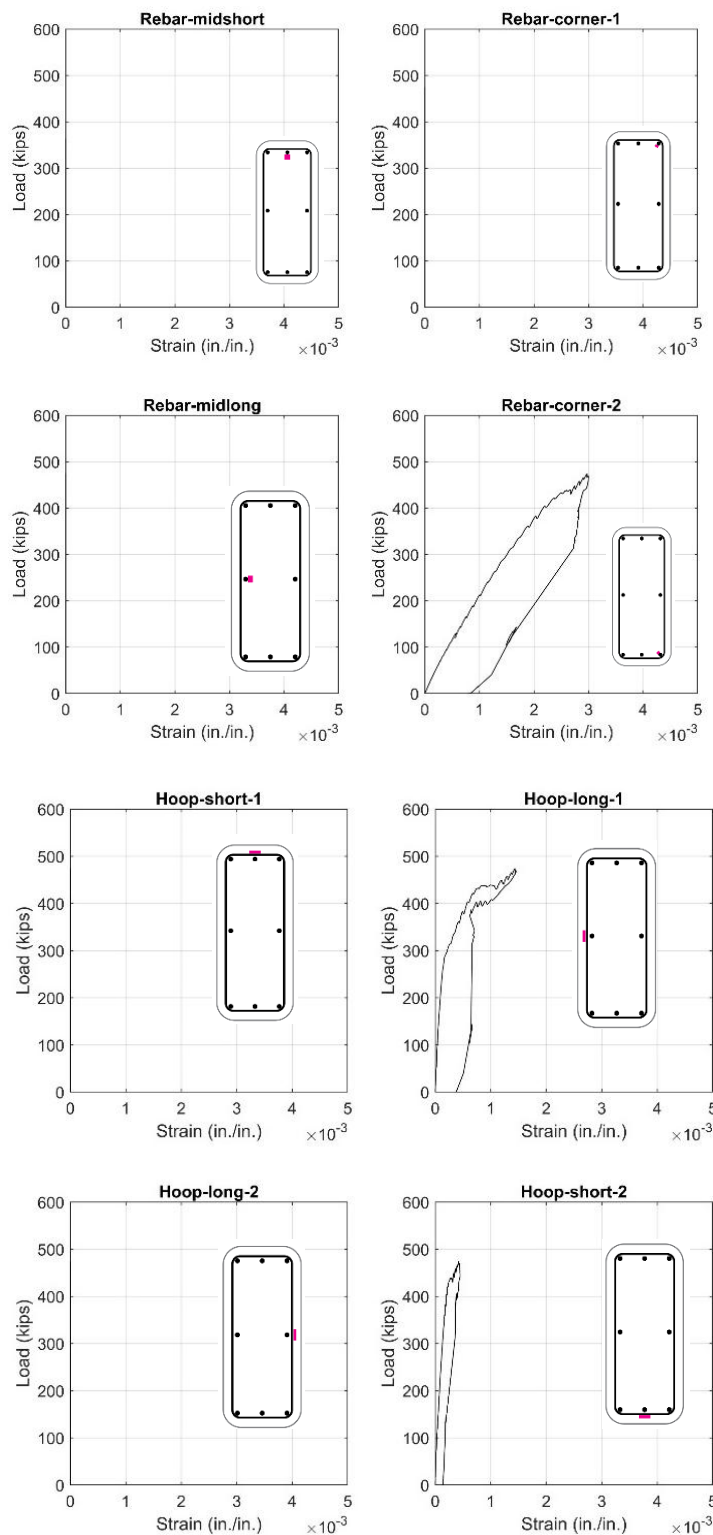


**Figure 37 Rebar strains for Group 4 Column 1.**

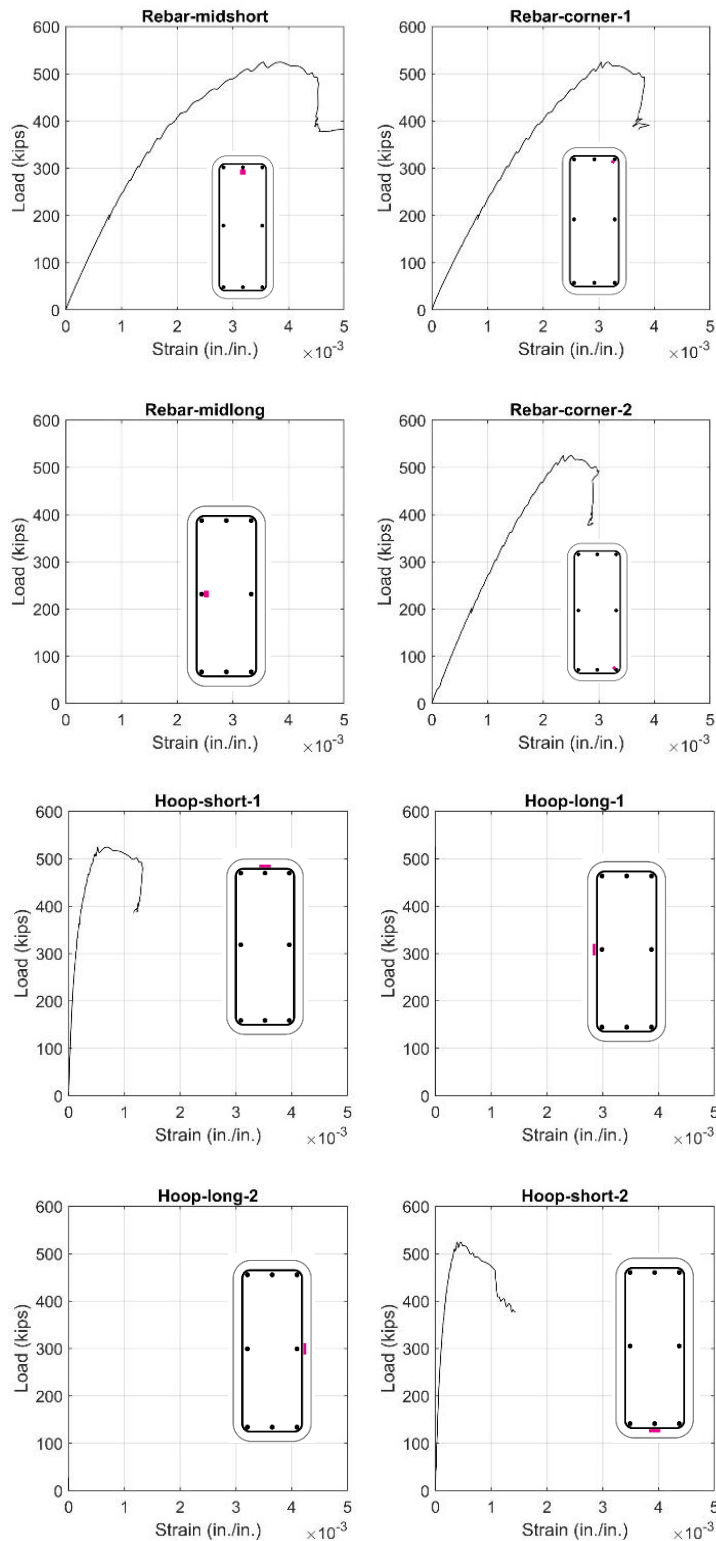


**Figure 38 Rebar strains for Group 4 Column 2.**

The FRP strains are presented in Figure 39. For both columns, the FRP strains on one side (FRP-2 for Column 1 and FRP-1 for Column 2 as shown in Figure 39) of the column exceeded 0.005 prior

to rupture, while the strains on the opposite side reached approximately 0.004. This indicates that the FRP strains in Group 4 were higher than those observed in Groups 2 and 3, aligning with the observation that the FRP provided greater confinement to the concrete upon reaching the peak load. Consequently, this demonstrates that through-FRP anchors can improve FRP confinement more effectively than part-through anchors. However, the Group 4 columns demonstrated a lower average peak load compared to Groups 2 and 3 columns. It remains unclear whether this was due to inter-group specimen variability, or the impact of the through-holes required for the through-anchors. Additional testing is needed to draw definitive conclusions.

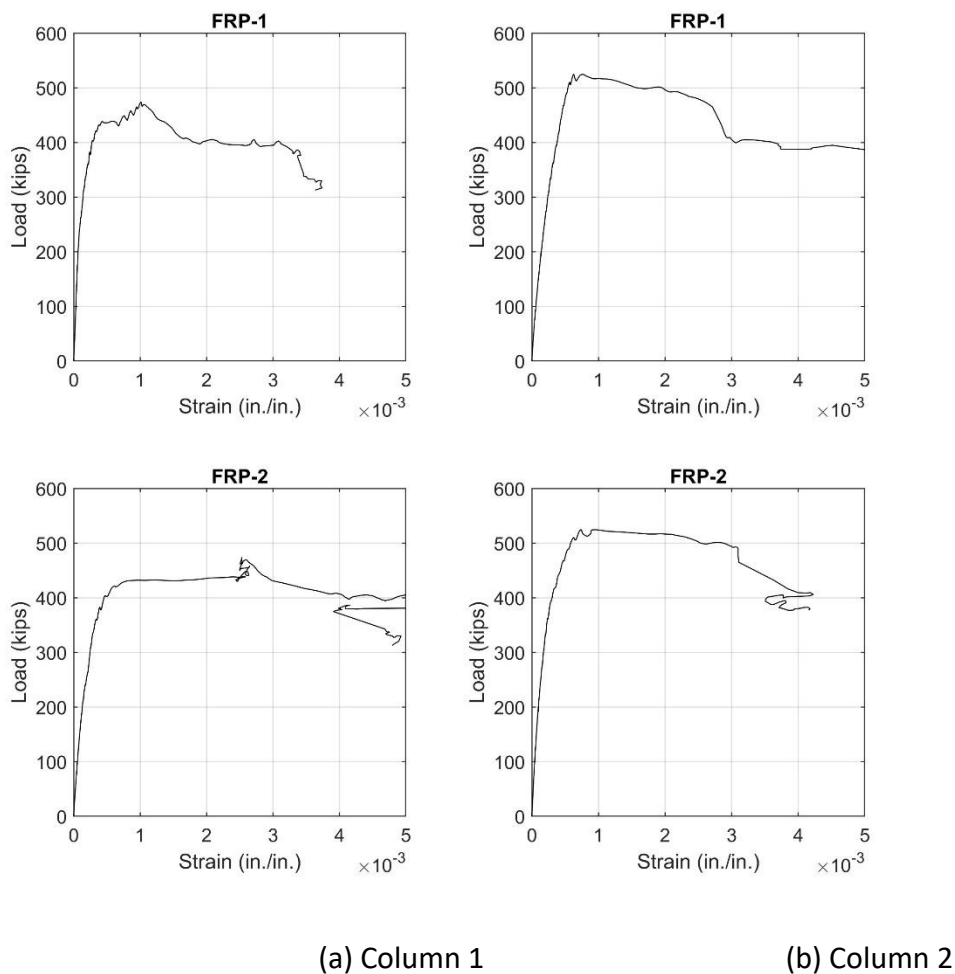


**Figure 39 FRP strains for Group 4 columns.**

## Group 5 results

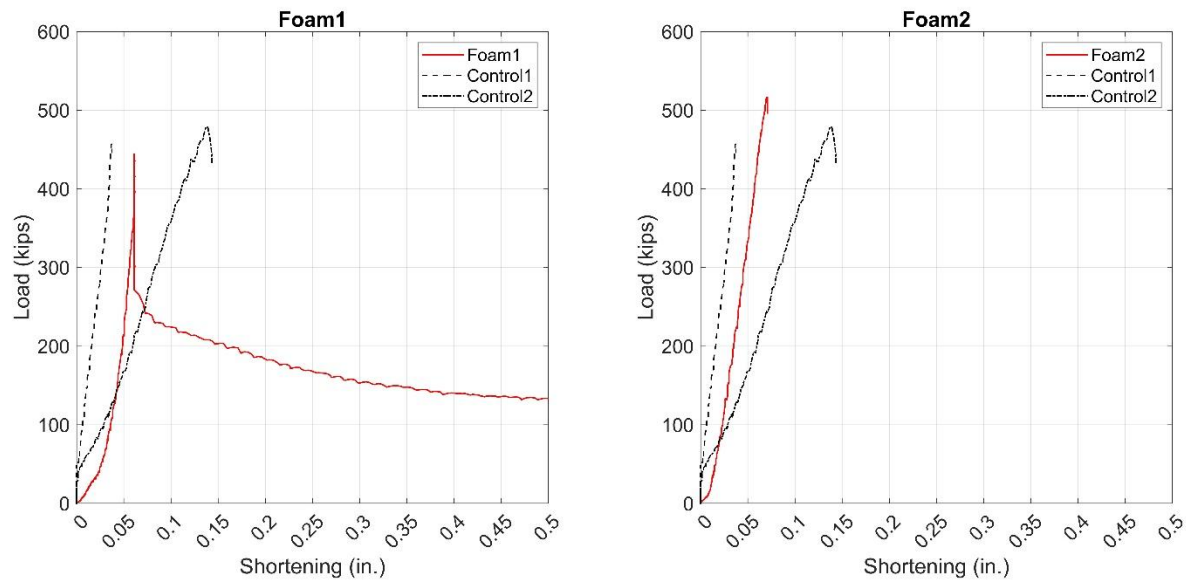
The failure mode of the Group 5 foam-profiled columns is illustrated in Figure 40. Both columns showed an identical failure, which was markedly different from all other groups. At the peak load, concrete crushing occurred with an audible noise, followed by a sudden drop in load. However,

no visible damage or deformation was observed on the surface of the FRP jacket. The columns continued to resist loading over a prolonged shortening without significant signs of damage or deformation. At very large shortening levels, some deformation of the FRP jacket became apparent, as shown in Figure 40, due to concrete dilation. Despite the large deformations, the columns were still able to carry load, and the test was terminated once significant deformation of the FRP jacket was observed.

The axial load versus load shortening curves for the Group 5 columns are presented in Figure 41, alongside those for the control columns for comparison. Following the initial load drop, the Group 5 columns displayed a sharp decline. For Column 2, the wood block to which the string potentiometer was attached fell off upon reaching the peak load, preventing further shortening measurements. However, Column 1 exhibited a gradual decrease in capacity as loading continued. In terms of peak load, Column 1 exhibited a slightly lower peak load compared to the control column, while Column 2 showed a slightly higher peak load. This variation is likely due to specimen variability, as no significant differences were observed between the two columns in Group 5.

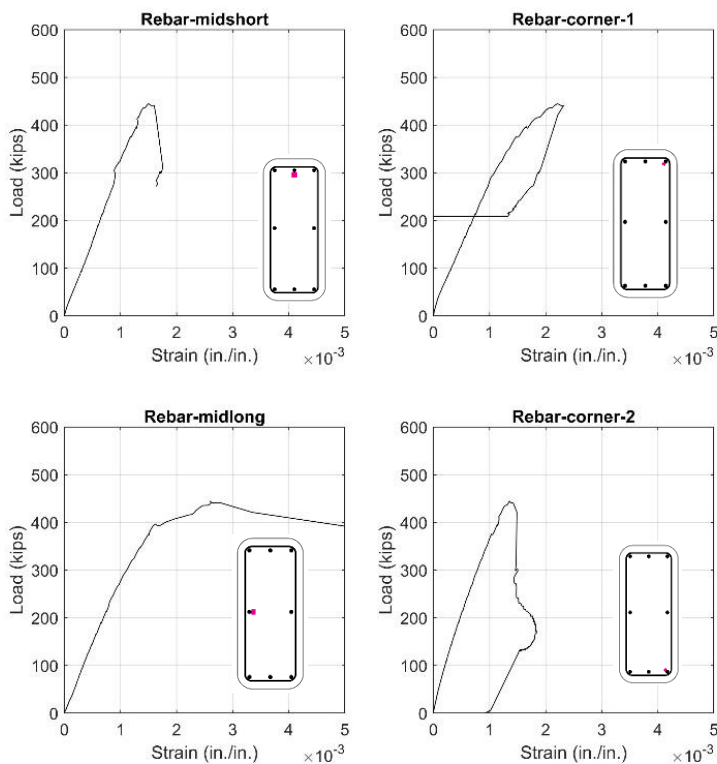


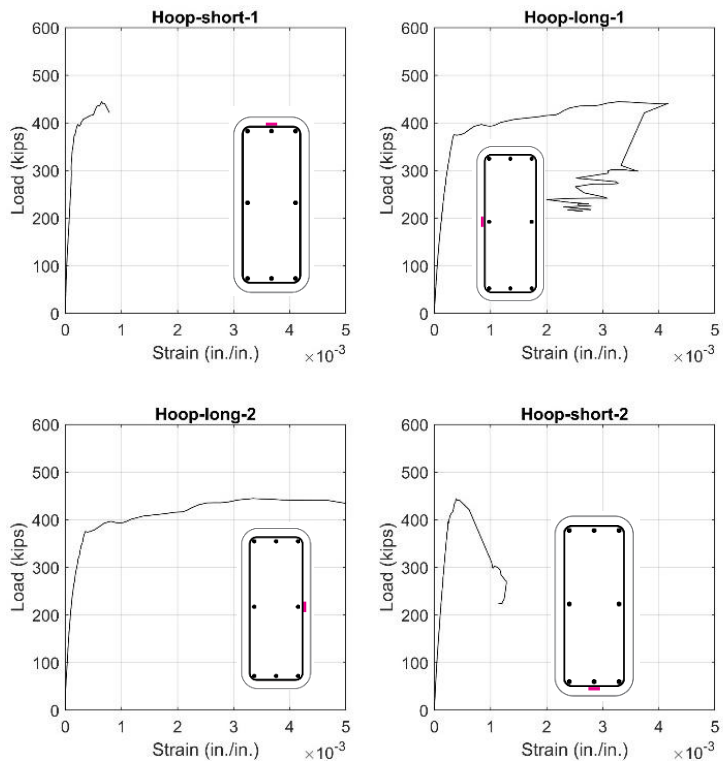
**Figure 40 Failure mode of Group 5 columns.**



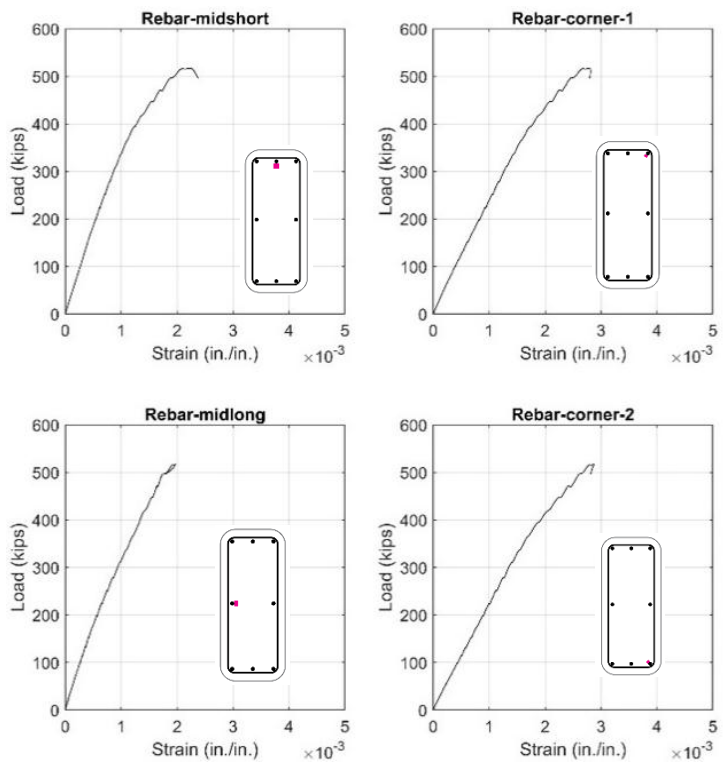
**Figure 41 Axial load versus axial shortening curves for Group 5 columns.**

The rebar strain data for Group 5 columns are presented in Figure 42 and Figure 43. The longitudinal rebar strain measurements indicate minimal yielding. The hoop strain measurements show evident tie yielding on the long side but not on the short side, similar to that of the control group.





**Figure 42 Rebar strains for Group 5 Column 1.**



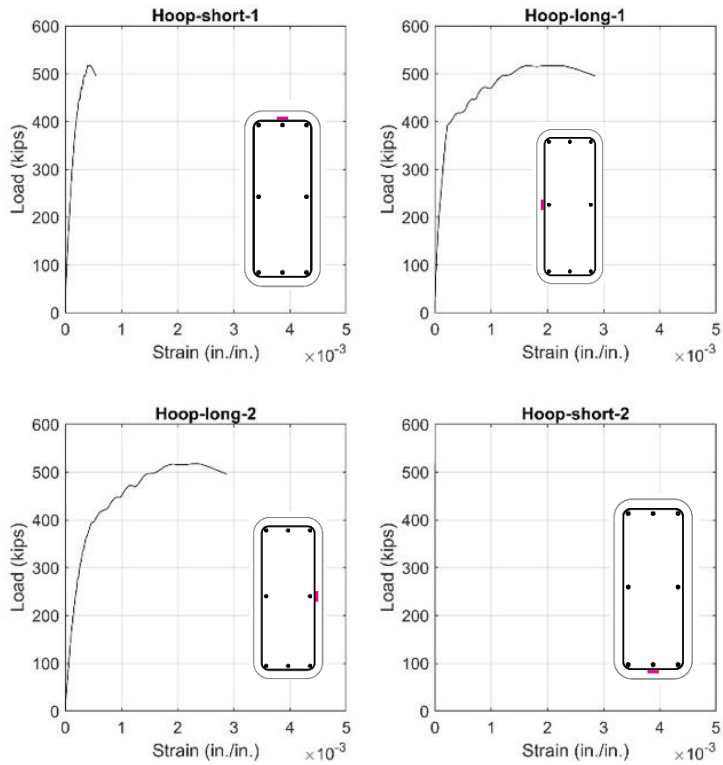


**Figure 43 Rebar strains for Group 5 Column 2.**

The FRP strains are presented in Figure 44. For Column 1, the FRP-2 strain reached approximately 0.003 prior to rupture, while the strain on the opposite side (FRP-1) reached around 0.002. In contrast, Column 2 showed no significant increase in FRP strain after reaching the peak load. This indicates that the FRP did not effectively confined the concrete beyond the peak load. This behavior is primarily attributed to the very low modulus of the geofoam, which deformed significantly under concrete dilation, resulting in limited engagement of the FRP in restraining the dilation.

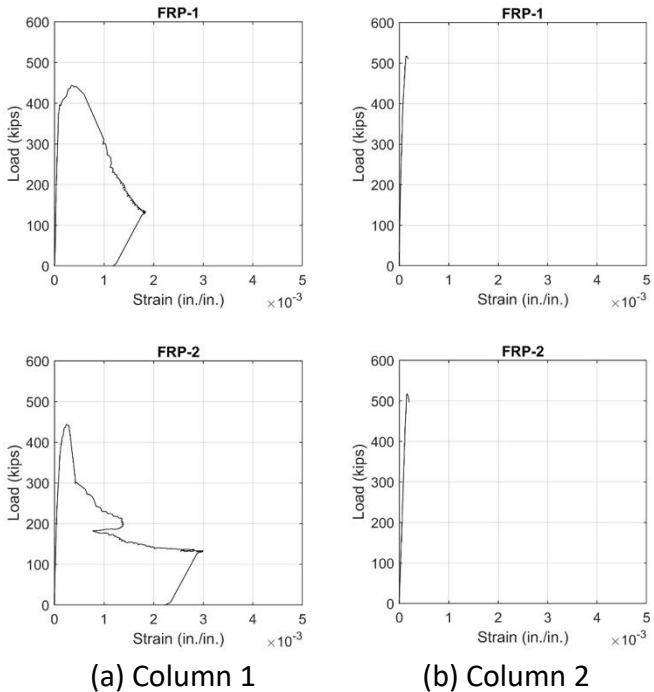


**Figure 44 FRP strains for Group 5 columns.**

## Group 6 results

The failure of Group 6 columns is illustrated in Figure 45 and Figure 46. Due to the unique design of this configuration, the FRP was unsupported by any surface during the fabrication process, see Figure 17 and Figure 18. Consequently, the two columns exhibited differences that are attributed to variability during installation. Column 1, shown in Figure 45, was fabricated with the FRP sheet flat and tightly wrapped. In contrast, the FRP on Column 2 displayed notable concavity, as shown in Figure 46.

This concavity affected the performance of Column 2, as the FRP was not fully engaged in confining the concrete from the beginning of the loading process. Instead, the FRP confinement contributed only after the concavity flattened during the later stages of loading, as shown in Figure 46. These fabrication differences also influenced the failure modes of the columns. Column 1 exhibited FRP rupture at the corner, while Column 2 showed no apparent FRP rupture throughout the loading process.

The axial load versus axial shortening curves for Group 6 columns are presented in Figure 47, alongside those for the control columns for comparison. After reaching the peak load, the Group 6 columns displayed a sharp decline. Subsequently, the columns continued carrying load as shortening occurred. Column 1 ultimately failed due to FRP rupture after considerable deformation. In contrast, Column 2 did not exhibit FRP rupture but experienced a second sudden drop in load, after which the test was terminated. Column 1 achieved the highest peak load among all columns, while Column 2 showed a significantly lower peak load, likely due to the concavity of the FRP jacket.

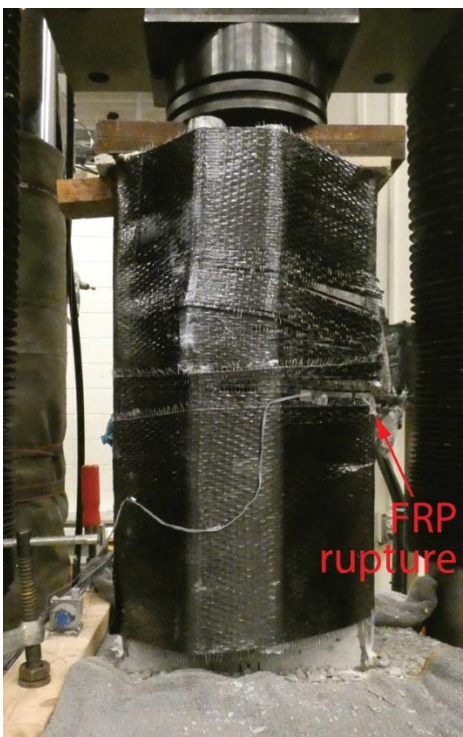


Figure 45 Failure mode of Group 6 Column 1.



(a) Before loading



(b) Close to failure

**Figure 46 Failure mode of Group 6 Column 2.**

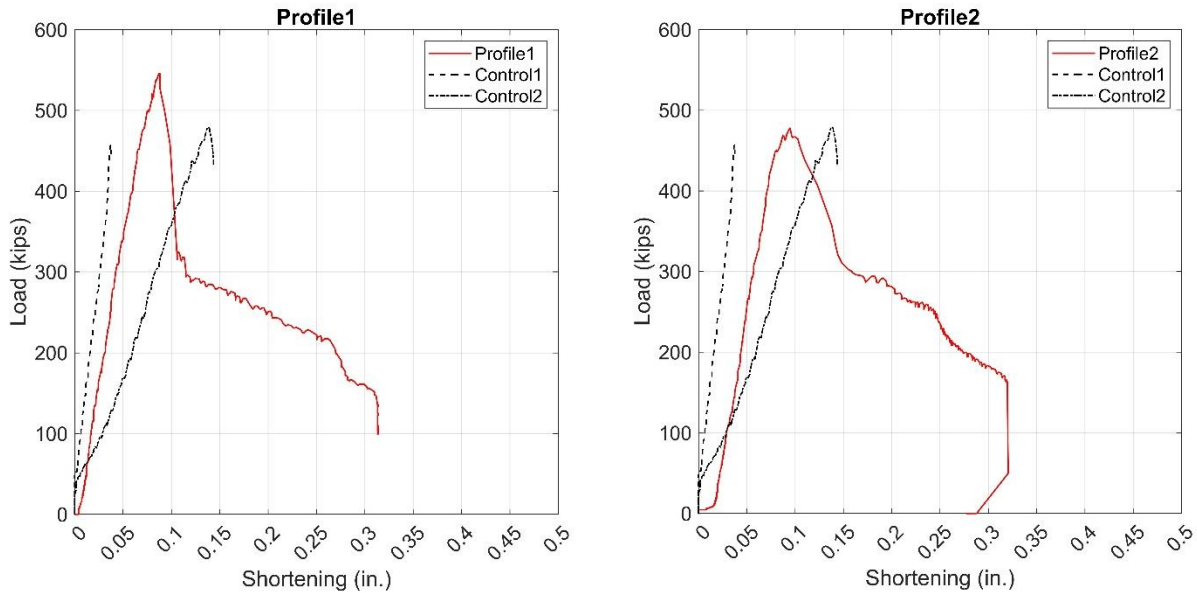


**Figure 47 Axial load versus axial shortening curves for Group 6 columns.**

The rebar strains for Group 6 columns are presented in Figure 48 and Figure 49. In Figure 49, the strain gauges at Rebar-corner-2, Hoop-short-1, Hoop-long-1, and Hoop-long-2 did not record any data, likely due to damage during concrete casting. The longitudinal rebar strain measurements indicate minimal yielding. Similarly, the hoop strain measurements show no evidence of tie yielding.

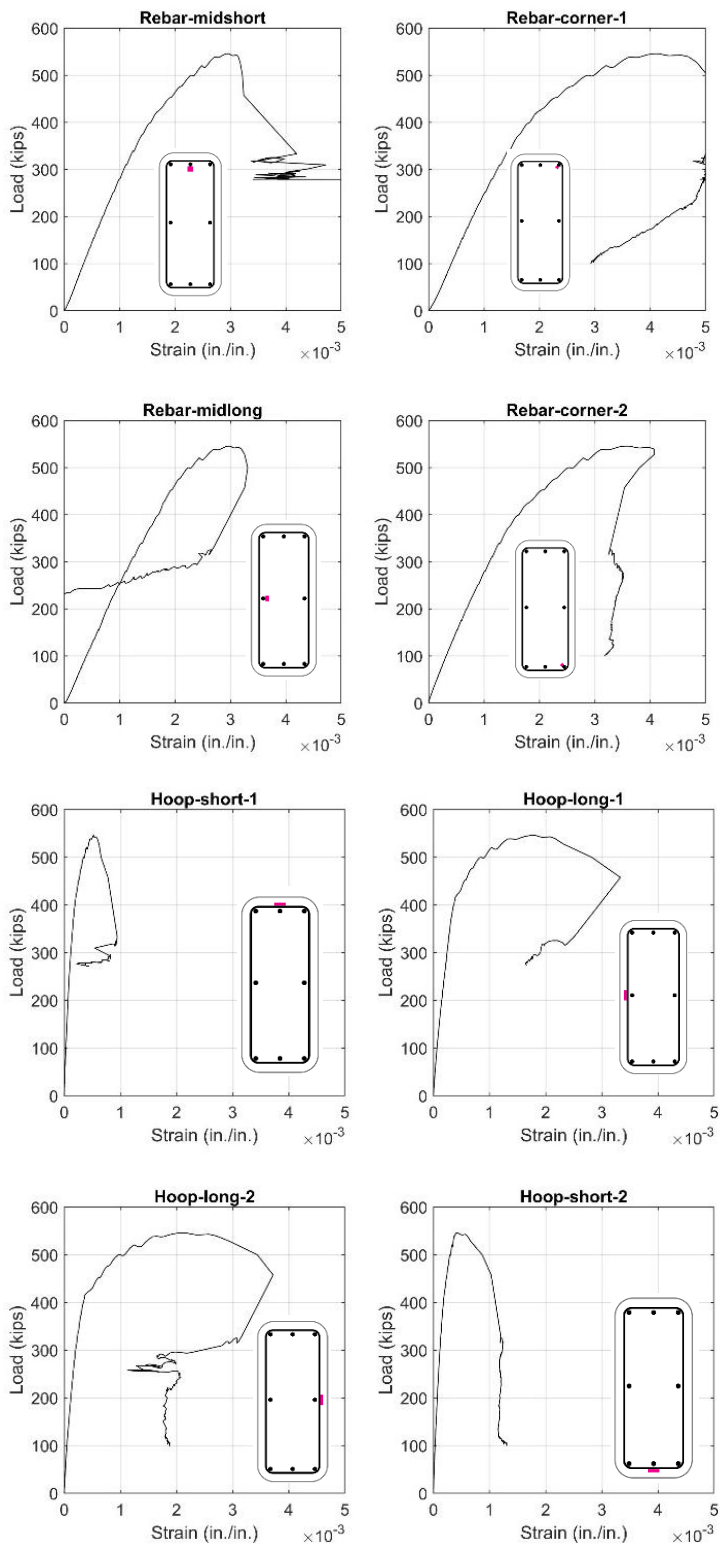


**Figure 48 Rebar strains for Group 6 Column 1.**

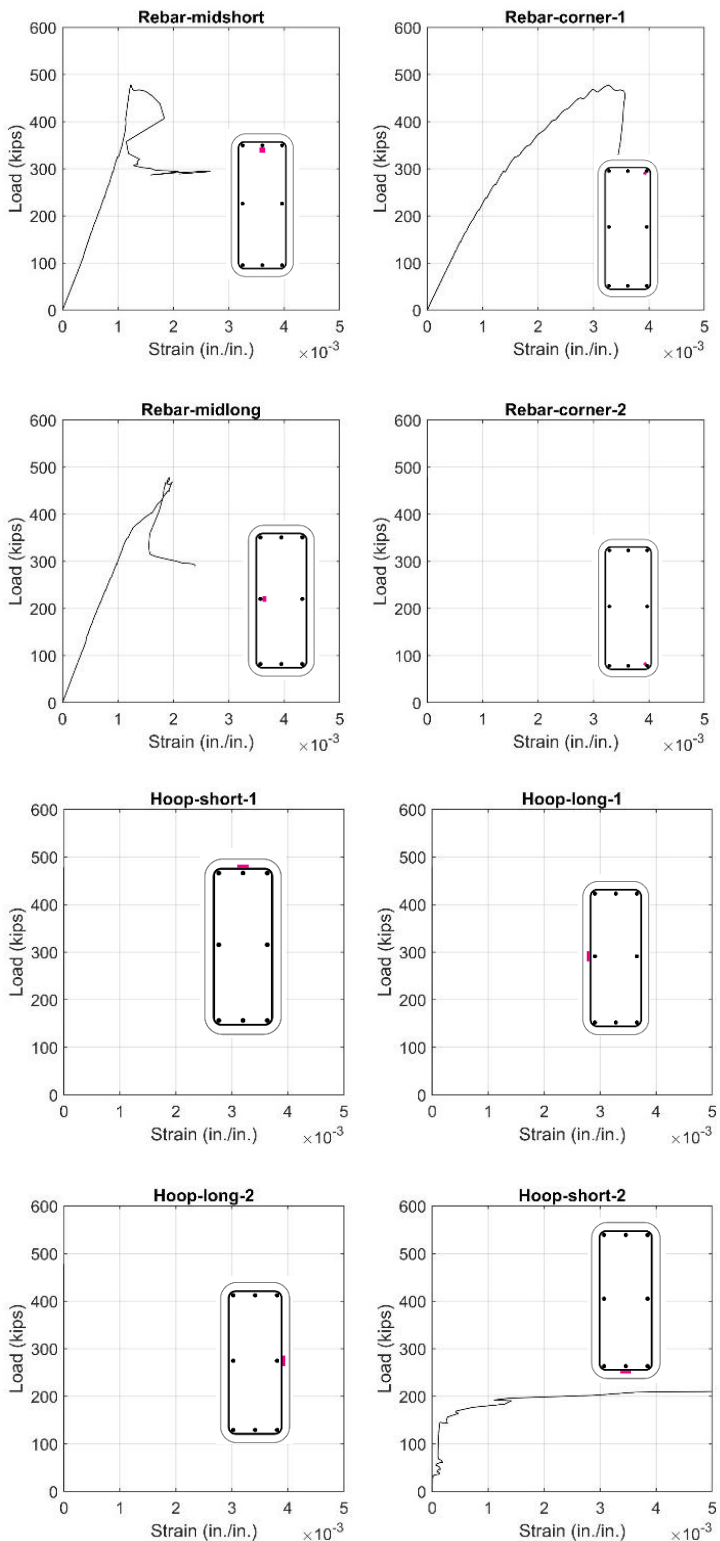


**Figure 49 Rebar strains for Group 6 Column 2.**

The FRP strains are presented in Figure 50. For both columns, the FRP strain on one side of the column (FRP-2 for Column 1 and FRP-1 for Column 2) exceeded 0.005 prior to failure, indicating

that the FRP effectively confined the concrete beyond the peak load. Prior to the peak load, Column 1 exhibited a higher FRP strain at peak load, reaching approximately 0.001 while Column 2 showed a lower FRP strain of about 0.0004 at peak load. This aligns with the observation that the concavity in the FRP wrap of Column 2 flattened at the later stages of loading, reducing the FRP's engagement in confinement.

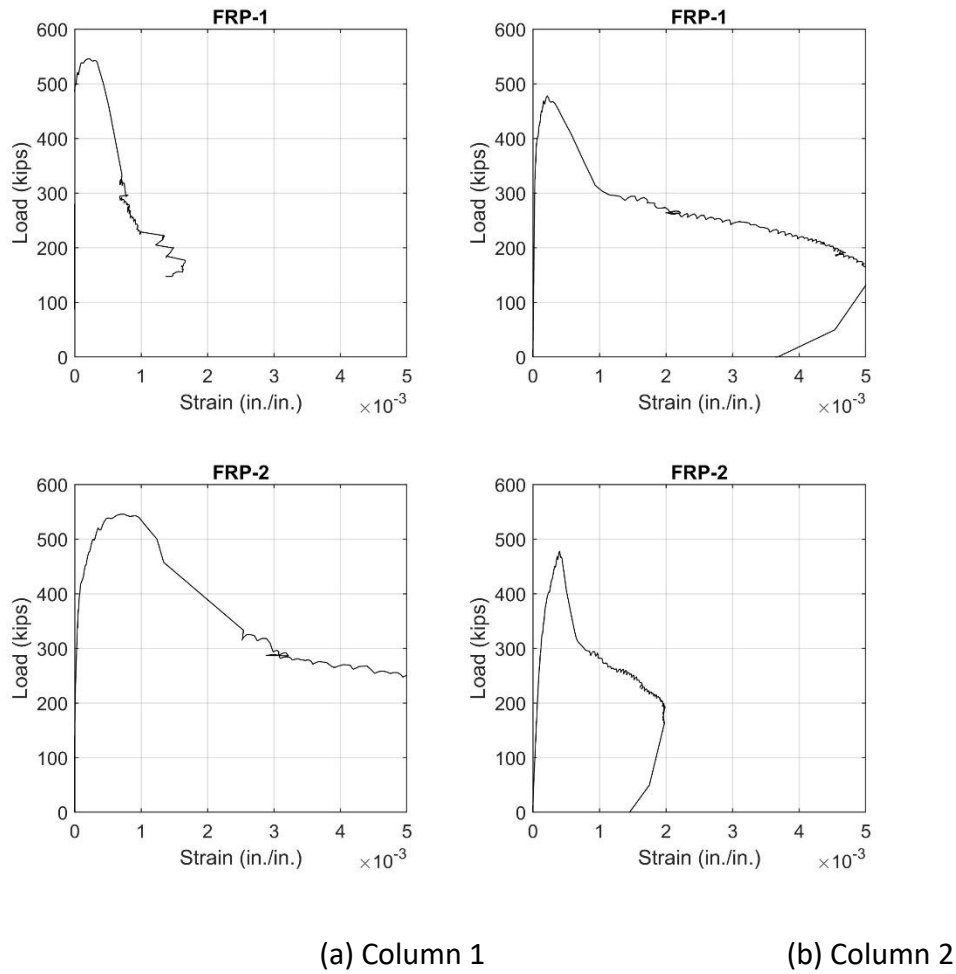


**Figure 50 FRP strains for Group 6 columns.**

## Summary of test results

The peak loads for all columns are summarized in Table 2, with a bar chart comparison provided in Figure 51. Based on the peak loads of Groups 2, 3, and 4, no significant enhancement was observed from the use of FRP anchors. For the geofoam-profiled Group 5 columns, the peak loads were lower than those of the Group 2 columns but slightly higher than those of the control group columns.

In contrast, the Group 6 steel tube-profiled columns exhibited substantial variation in performance. Column 1 showed the highest enhancement, with a 16.5% increase in peak load, while Column 2 showed only 2.1% increase, primarily due to fabrication flaws. These results suggest that combining geofoam and steel tubes offers a promising approach to enhancing the effectiveness of FRP confinement. The geofoam provides a solid surface for the FRP to be flat and tightly wrapped around the column, while the steel tube offers sufficient stiffness to engage the FRP in confining the concrete rather than deforming under the low-modulus geofoam. However, further experiments are needed to better understand the mechanisms and effects of this combined system.

**Table 2 Summary of load capacity of all columns.**

Group	Column	Peak load (kips)	Improvement Over Group 1		Improvement Over Group 2	
1	1	457	N.A.	N.A.	N.A.	N.A.
	2	479	N.A.		N.A.	
2	1	528	12.7%	11.8%	N.A.	N.A.
	2	518	10.6%		N.A.	
3	1	515	10.0%	12.0%	-1.5%	0.2%
	2	533	13.9%		1.9%	
4	1	474	1.3%	6.7%	-9.4%	-4.5%
	2	525	12.1%		0.4%	
5	1	444	-5.0%	2.7%	-15.1%	-8.1%
	2	517	10.4%		-1.1%	
6	1	546	16.6%	9.4%	4.4%	-2.1%
	2	478	2.1%		-8.6%	

### TASK 3: Comparative analysis of test data against published data in the literature

A literature review was conducted to understand the existing research on FRP-confined rectangular concrete columns. With this understanding, the experimental data generated in this project can be put into context and hence the performance of the proposed FRP strengthening strategies can be evaluated.

Within the topic of FRP-confined rectangular concrete columns, existing studies can be categorized as follows with respect to the characteristics of the concrete column and the FRP confinement:

- Plain short concrete columns reinforced with wet layup FRP jackets.
- Plain short concrete columns reinforced with prefabricated FRP tubes.

- Reinforced concrete columns reinforced with wet layup FRP jackets.
- Reinforced concrete columns reinforced with prefabricated FRP tubes.
- FRP-confined concrete columns under concentric compression.
- FRP-confined concrete columns under eccentric compression.
- Columns with a square cross-section.
- Columns with a rectangular cross-section.
- Columns with normal strength concrete.
- Columns with high strength concrete.
- Columns with ultra-high performance concrete (UHPC).
- Columns confined with carbon FRP (CFRP).
- Columns confined with glass FRP (GFRP).

For the purpose of the current project, all studies except for the ones with circular and elliptical cross-sections were reviewed. Additionally, specimens tested under eccentric compression were excluded. A total of 24 studies were screened as listed below.

- [1] Pessiki, S., K. A. Harries, J. T. Kestner, R. Sause, and J. M. Ricles. 2001. "Axial Behavior of Reinforced Concrete Columns Confined with FRP Jackets." *J. Compos. Constr.*, 5 (4): 237–245. [https://doi.org/10.1061/\(ASCE\)1090-0268\(2001\)5:4\(237\)](https://doi.org/10.1061/(ASCE)1090-0268(2001)5:4(237)).
- [2] Rousakis, T. C., A. I. Karabinis, and P. D. Kiousis. 2007. "FRP-confined concrete members: Axial compression experiments and plasticity modelling." *Engineering Structures*, 29 (7): 1343–1353. <https://doi.org/10.1016/j.engstruct.2006.08.006>.
- [3] Wang, L.-M., and Y.-F. Wu. 2008. "Effect of corner radius on the performance of CFRP-confined square concrete columns: Test." *Engineering Structures*, 30 (2): 493–505. <https://doi.org/10.1016/j.engstruct.2007.04.016>.
- [4] Masia, M. J., T. N. Gale, and N. G. Shrive. 2004. "Size effects in axially loaded square-section concrete prisms strengthened using carbon fibre reinforced polymer wrapping." *Can. J. Civ. Eng.*, 31 (1): 1–13. <https://doi.org/10.1139/l03-064>.
- [5] Al-Salloum, Y. A. 2007. "Influence of edge sharpness on the strength of square concrete columns confined with FRP composite laminates." *Composites Part B: Engineering*, 38 (5–6): 640–650. <https://doi.org/10.1016/j.compositesb.2006.06.019>.

- [6] Zeng, J.-J., J. Liao, D.-H. Zhu, and P.-D. Li. 2023. "Axial compressive behavior and design-oriented model for large-rupture-strain (LRS) FRP-confined concrete in rectangular columns." *Journal of Building Engineering*, 75: 106925. <https://doi.org/10.1016/j.jobe.2023.106925>.
- [7] Ozbakkaloglu, T. 2013a. "Axial Compressive Behavior of Square and Rectangular High-Strength Concrete-Filled FRP Tubes." *J. Compos. Constr.*, 17 (1): 151–161. [https://doi.org/10.1061/\(ASCE\)CC.1943-5614.0000321](https://doi.org/10.1061/(ASCE)CC.1943-5614.0000321).
- [8] Toutanji, H. A., M. Han, and S. Matthys. 2007. "AXIAL LOAD BEHAVIOR OF RECTANGULAR CONCRETE COLUMNS CONFINED WITH FRP COMPOSITES."
- [9] Rochette, P., and P. Labossière. 2000. "Axial Testing of Rectangular Column Models Confined with Composites." *J. Compos. Constr.*, 4 (3): 129–136. [https://doi.org/10.1061/\(ASCE\)1090-0268\(2000\)4:3\(129\)](https://doi.org/10.1061/(ASCE)1090-0268(2000)4:3(129)).
- [10] Zeng, J. J., G. Lin, J. G. Teng, and L. J. Li. 2018. "Behavior of large-scale FRP-confined rectangular RC columns under axial compression." *Engineering Structures*, 174: 629–645. <https://doi.org/10.1016/j.engstruct.2018.07.086>.
- [11] Wang, Y., P. Liu, Q. Cao, G. Chen, B. Wan, Z. Wei, and Y.-L. Bai. 2021. "Comparison of monotonic axial compressive behavior of rectangular concrete confined by FRP with different rupture strains." *Construction and Building Materials*, 299: 124241. <https://doi.org/10.1016/j.conbuildmat.2021.124241>.
- [12] Saleem, S., Q. Hussain, and A. Pimanmas. 2017. "Compressive Behavior of PET FRP–Confined Circular, Square, and Rectangular Concrete Columns." *J. Compos. Constr.*, 21 (3): 04016097. [https://doi.org/10.1061/\(ASCE\)CC.1943-5614.0000754](https://doi.org/10.1061/(ASCE)CC.1943-5614.0000754).
- [13] Ozbakkaloglu, T., and D. J. Oehlers. 2008. "Concrete-Filled Square and Rectangular FRP Tubes under Axial Compression." *J. Compos. Constr.*, 12 (4): 469–477. [https://doi.org/10.1061/\(ASCE\)1090-0268\(2008\)12:4\(469\)](https://doi.org/10.1061/(ASCE)1090-0268(2008)12:4(469)).
- [14] Chen, L., and T. Ozbakkaloglu. 2016. "Corner strengthening of square and rectangular concrete-filled FRP tubes." *Engineering Structures*, 117: 486–495. <https://doi.org/10.1016/j.engstruct.2016.03.031>.
- [15] Abbasnia, R., F. Hosseinpour, M. Rostamian, and H. Ziaadiny. 2013. "Cyclic and monotonic behavior of FRP confined concrete rectangular prisms with different aspect ratios." *Construction and Building Materials*, 40: 118–125. <https://doi.org/10.1016/j.conbuildmat.2012.10.008>.
- [16] Lam, L., and J. G. Teng. 2003. "Design-Oriented Stress-Strain Model for FRP-Confined Concrete in Rectangular Columns." *Journal of Reinforced Plastics and Composites*, 22 (13): 1149–1186. <https://doi.org/10.1177/0731684403035429>.

- [17] Wu, Y.-F., and Y.-Y. Wei. 2010. "Effect of cross-sectional aspect ratio on the strength of CFRP-confined rectangular concrete columns." *Engineering Structures*, 32 (1): 32–45. <https://doi.org/10.1016/j.engstruct.2009.08.012>.
- [18] Micelli, F., and R. Modarelli. 2013. "Experimental and analytical study on properties affecting the behaviour of FRP-confined concrete." *Composites Part B: Engineering*, 45 (1): 1420–1431. <https://doi.org/10.1016/j.compositesb.2012.09.055>.
- [19] Wei, Y., Y. Zhang, J. Chai, G. Wu, and Z. Dong. 2020. "Experimental investigation of rectangular concrete-filled fiber reinforced polymer (FRP)-steel composite tube columns for various corner radii." *Composite Structures*, 244: 112311. <https://doi.org/10.1016/j.compstruct.2020.112311>.
- [20] Ilki, A., O. Peker, E. Karamuk, C. Demir, and N. Kumbasar. 2008. "FRP Retrofit of Low and Medium Strength Circular and Rectangular Reinforced Concrete Columns." *J. Mater. Civ. Eng.*, 20 (2): 169–188. [https://doi.org/10.1061/\(ASCE\)0899-1561\(2008\)20:2\(169\)](https://doi.org/10.1061/(ASCE)0899-1561(2008)20:2(169)).
- [21] Chen, G., J. Zhang, Y. Wu, G. Lin, and T. Jiang. 2021. "Stress–Strain Behavior of FRP-Confining Recycled Aggregate Concrete in Square Columns of Different Sizes." *J. Compos. Constr.*, 25 (5): 04021040. [https://doi.org/10.1061/\(ASCE\)CC.1943-5614.0001150](https://doi.org/10.1061/(ASCE)CC.1943-5614.0001150).
- [22] Farghal, O. A. 2018. "Structural performance of axially loaded FRP-confined rectangular concrete columns as affected by cross-section aspect ratio." *HBRC Journal*, 14 (3): 264–271. <https://doi.org/10.1016/j.hbrcj.2016.11.002>.
- [23] Zhu, J. Y., G. Lin, J.-G. Teng, T.-M. Chan, J.-J. Zeng, and L.-J. Li. 2020. "FRP-Confined Square Concrete Columns with Section Curvilinearization under Axial Compression." *J. Compos. Constr.*, 24 (2): 04020004. [https://doi.org/10.1061/\(ASCE\)CC.1943-5614.0000999](https://doi.org/10.1061/(ASCE)CC.1943-5614.0000999).
- [24] Cao, Y., Y. Liu, X. Li, and Y. Wu. 2023. "Axial stress strain behavior of FRP-confined rectangular rubber concrete columns with different aspect ratio." *Engineering Structures*, 297: 116987. <https://doi.org/10.1016/j.engstruct.2023.116987>.

In these 24 studies conducted between 2001 and 2023, a total of 406 FRP-confined concrete columns were tested, covering a wide range of geometries, material properties, and confinement configurations. The design details and test results from these studies were compiled into a database, which is provided as an Excel file attached to this report. This database serves as a comprehensive literature review, summarizing key parameters that influence the confinement behavior of FRP-wrapped concrete columns. **The database is attached to this report as an excel file.**

The database records essential geometric properties of the tested columns, including overall dimensions, cross-sectional aspect ratios (square or rectangular), and the ratio of the corner radius to the section's width. Among the compiled specimens, the cross-section dimensions vary significantly, with widths ranging from 100 mm to 500 mm and corresponding heights extending

up to 600 mm. The length-to-width ratio was systematically recorded, with the majority of studies focusing on ratios between 1.0 and 2.5, reflecting the typical range for structural columns. Notably, while data for columns with a 2.5 cross-section aspect ratio remains scarce, several studies provide results for 2.0 aspect ratio columns, which can serve as a comparative reference.

For concrete, the database provides critical material properties, including the uniaxial compressive strength, which ranges from 15 MPa to over 90 MPa, covering normal- to high-strength concrete applications. Additionally, the compressive strain at peak strength is documented, offering insights into the ductility of unconfined concrete in comparison to confined specimens.

The FRP confinement characteristics are extensively detailed, capturing key parameters such as the FRP elastic modulus, which spans from 65 GPa to 240 GPa, depending on the fiber type and resin system. Experimental test results documented in the database include the average cross-sectional failure strength and the corresponding axial strain at peak load. By comparing these values to their unconfined counterparts, the database facilitates an assessment of the confinement effectiveness of FRP. The ratio of confined-to-unconfined compressive strength and the ratio of confined-to-unconfined strain are key indicators of how FRP confinement enhances both the load-carrying capacity and ductility of concrete columns.

A detailed analysis comparing the test results from this project with the data available in the database will be conducted as part of a planned journal paper. This comparative study will contextualize the improvement in axial capacity provided by the FRP systems tested in this project by considering factors such as concrete cross-section stiffness and FRP material properties. Given the limited availability of test data for columns with a 2.5 aspect ratio, this study will also explore trends observed in 2.0 aspect ratio columns, providing a broader perspective on the influence of geometric proportions on FRP confinement performance.

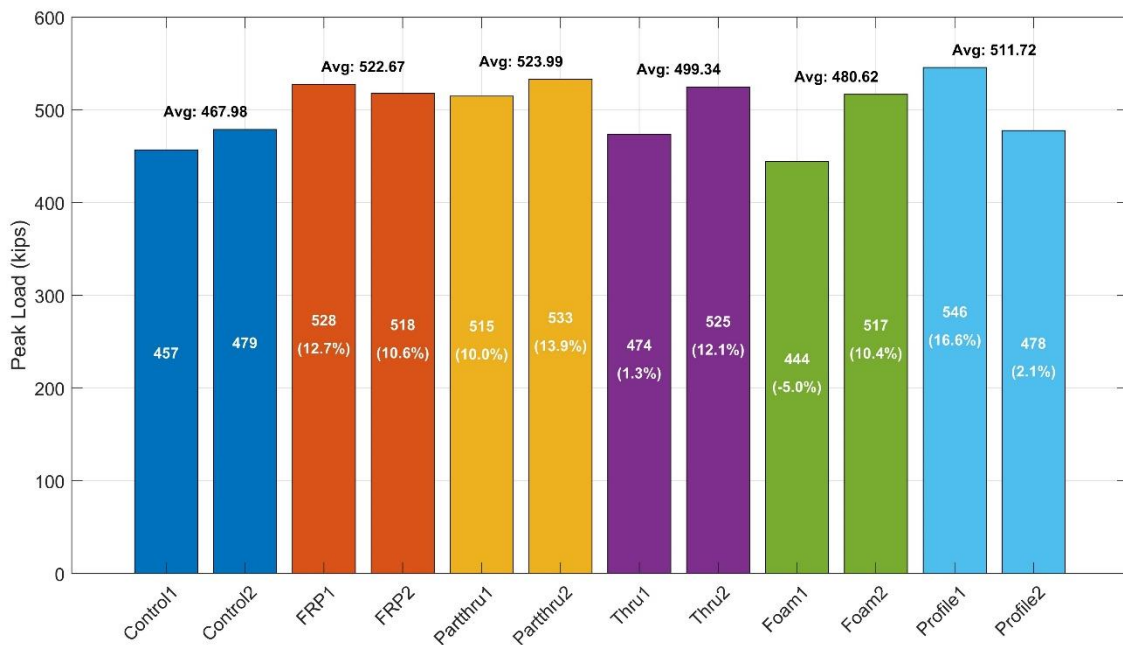


**Figure 51 Summary of peak load of all columns.**

## CONCLUSIONS AND RECOMMENDATIONS FOR FUTURE RESEARCH

Based on the experimental data, the following conclusions were drawn.

The application of direct FRP jacketing led to an average capacity increase of 11.7% for the columns tested in this study. This increase demonstrates the effectiveness of FRP jacketing in enhancing the load-carrying capacity of rectangular concrete columns.

Ineffectiveness of FRP Anchoring Systems: contrary to expectations, the incorporation of both part-through and through FRP anchoring systems did not result in a significant capacity improvement beyond those achieved with direct FRP jacketing alone. This suggests that FRP anchoring systems may be ineffective for column configurations with large aspect ratios and traditional jacketing methods.

Geofoam Profiling System: the geofoam-based profiling system did not show any notable improvement compared to the direct FRP group. In fact, it resulted in an average capacity decrease. This outcome is primarily attributed to the low stiffness of the geofoam, which failed to provide adequate support for improving the confinement of the concrete by the FRP jacket.

Steel Tube Profiling System: the steel tube profiling system exhibited large variability between the two columns tested. One specimen demonstrated an increase in capacity of 16.6%, surpassing the average improvement observed with direct FRP jacketing. The variability was largely due to a slack in the FRP jacket that occurred during installation, which critically affected

the effectiveness of the confinement. Notably, even for the specimen with a 16.6% increase in capacity, the FRP jacket was not perfectly flat, indicating potential for further improvement if flatness is controlled.

Recommendations for Future Research: to build upon these findings, the following recommendations are made.

**Development and Testing of a Hybrid Profiling System:** a hybrid FRP profiling system that combines the geofoam and steel tube components is recommended for further investigation. In this system, the geofoam will serve as a base to create a flat surface, ensuring uniform application of the FRP jacket. Despite its low stiffness, geofoam is sufficient to maintain surface flatness. Steel tubes provide structural support, enhancing the confinement effect by effectively transmitting confining forces as the concrete core dilates under load.

**Experimental Program Design:** to evaluate the performance of this hybrid system, a comprehensive experimental program should be designed, including a control group with unconfined columns serving as a baseline for comparison, a direct FRP group with standard FRP jacketing to assess the baseline effectiveness of the technique, and a hybrid group utilizing the proposed hybrid profiling system. Within this hybrid group, multiple sub-groups should be tested to explore the effects of varying parameters such as support stiffness, profiled section dimensions, concrete surface preparation (size and locations of holes), installation methods, and FRP jacket configurations.

This study provided valuable insights into the performance of different FRP strengthening techniques for rectangular concrete columns with a high cross-sectional aspect ratio. Based on the direct FRP jacketing effectiveness, anchoring systems and geofoam profiling alone do not offer additional benefits for the specific configurations tested here. The proposed hybrid system presents a promising avenue for future research, with the potential to significantly enhance the effectiveness of confinement and structural capacity of FRP-strengthened rectangular columns. Continued exploration and optimization of this system will contribute to more robust, cost-effective, and reliable retrofitting solutions in structural engineering applications.

# Data Management Plan

## **Products of Research**

This project involves the development of an effective FRP strengthening system for rectangular concrete columns. Finite element analysis will be used to design the proposed FRP system, and an experimental program will be conducted to evaluate the effectiveness of the system. Data will be produced as a result of the computational and experimental studies. Data from computer simulations will be in the form of input files for the software, output files (mostly text) and rendered images. From experiments, we will obtain data in the form of text, spreadsheets, and digital image files.

## **Data Format and Content**

Data generated in this project will be in the following formats: ASCII text (files from testing equipment), jpeg (photos from experiments), MS Word (test results and technical papers), MS Power Point (meeting presentations), MS Excel (literature review, data processing sheets), and PDF (technical papers, test results).

## **Data Access and Sharing**

The PI and Co-PI of this project are committed to the dissemination of data generated in this work to the public. The data collected or generated during the course of this project, the data descriptions and schema will be submitted to the PSR Director for review. Upon any revisions requested by the PSR Director, the data, data descriptions and schema will be submitted to the open data publishing platform Dryad by the PI and available to the public.

## **Reuse and Redistribution**

The data generated from this project will be made available to the general public for reuse and redistribution. Users are permitted to copy, distribute, and adapt the data for any purpose, including commercial use, provided proper attribution is given to the original source.

Any modifications or derivative works created from the data should clearly indicate changes from the original dataset. Users are responsible for ensuring compliance with all applicable laws and ethical guidelines when reusing the data. No warranties are provided regarding the accuracy, completeness, or fitness of the data for any particular purpose.

The research data can be accessed through the below link:

[https://www.dropbox.com/scl/fo/i5dcld70fk7dr65jdlws2o/AArWfnEyNThRVbg\\_ErZx58E?rlkey=xvd5w907txjvjgegy14ovyg7&dl=0](https://www.dropbox.com/scl/fo/i5dcld70fk7dr65jdlws2o/AArWfnEyNThRVbg_ErZx58E?rlkey=xvd5w907txjvjgegy14ovyg7&dl=0)